

## Comparison between Interior Layered Deposits in Valles Marineris and Terrestrial Sub-ice Volcanoes

---

The interior layered deposit mounds or ILDs in Valles Marineris are compositionally and morphologically similar to many terrestrial basaltic tuyas and the ILD-containing chasmata either lead to outflow channels or show signs of water (over-)flow on the adjoining plateau surfaces. Because the significant weaknesses inherent in alternative interpretations, many workers have suggested that the ILDs may be sub-ice volcanoes (Croft, 1990; Lucchitta et al., 1994; Chapman and Tanaka, 2001; Komatsu et al., 2003). Although the hypothesis that the ILDs are sub-ice volcanoes is not new, there is a paucity of comparative planetary studies of sub-ice volcanoes using terrestrial examples and MOC imagery of the ILDs. In order to test the subglacial volcanic hypothesis for ILDs, an ongoing study has investigated terrestrial sub-ice volcanoes and compared them to characteristics of analog ILDs on Mars. In doing so, we have found several commonalities that suggest comparable volcanic processes.

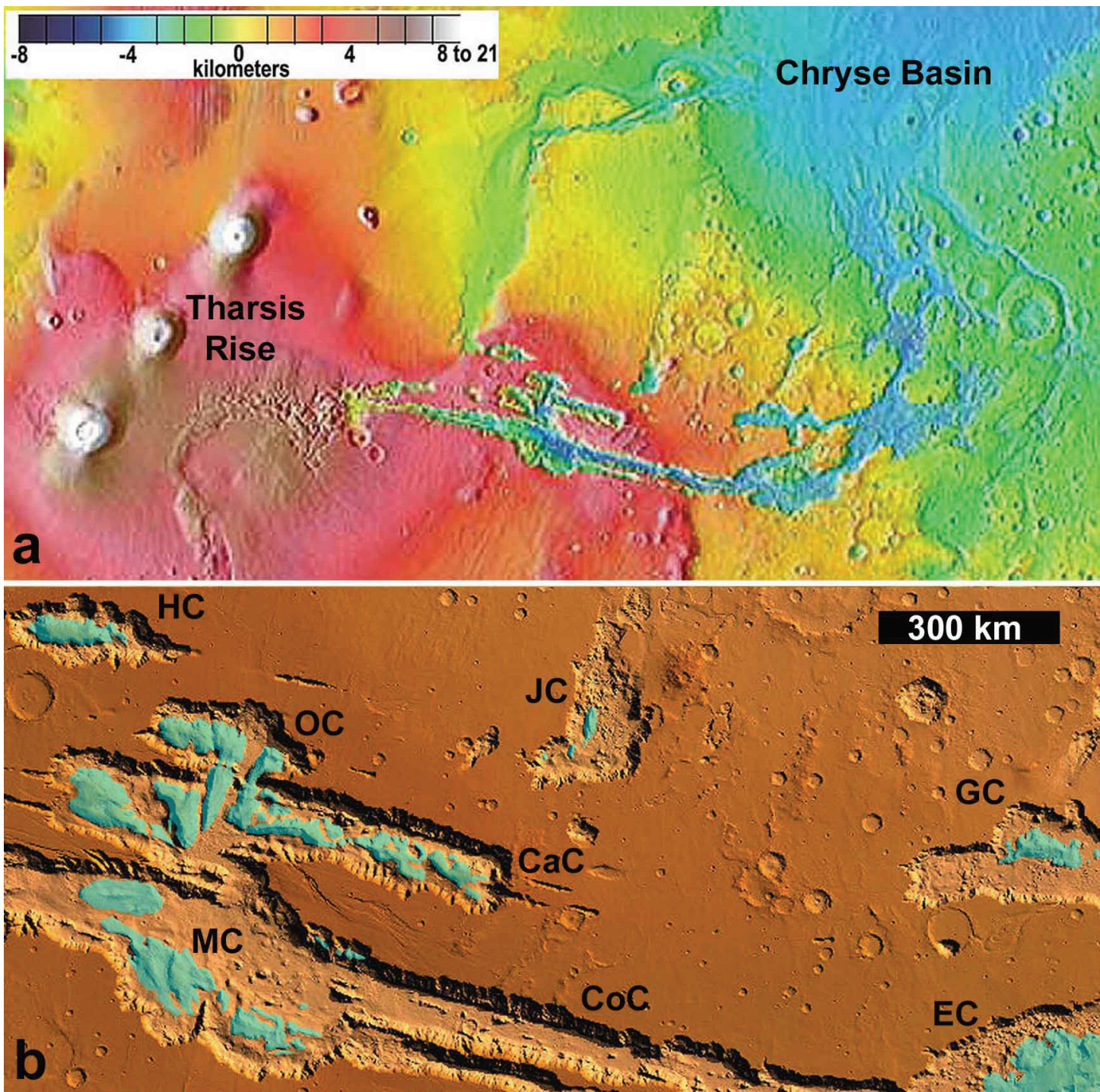


Figure 1: Views of the 3,000-km-long canyon of Valles Marineris, Mars. (a) MOLA (Mars Observer Laser Altimeter) topographic view showing volcanoes of the Tharsis Rise, on the west, to catastrophic flood channels that drain into Chryse Basin from Valles Marineris, on the east; (b) MOLA derived 3-dimensional enlarged view of central and east Valles Marineris showing interior layered deposits in blue (HC = Hebes Chasma, OC = Ophir Chasma, CaC = Candor Chasma, MC = Melas Chasma, CoC = Coprates Chasma, JC = Juventae Chasma, GC = Gangis Chasma, and EC = Eos Chasma); note topographic lows in central Melas and Juventae Chasma on (a); ILDs in Tithonium Chasma not shown.

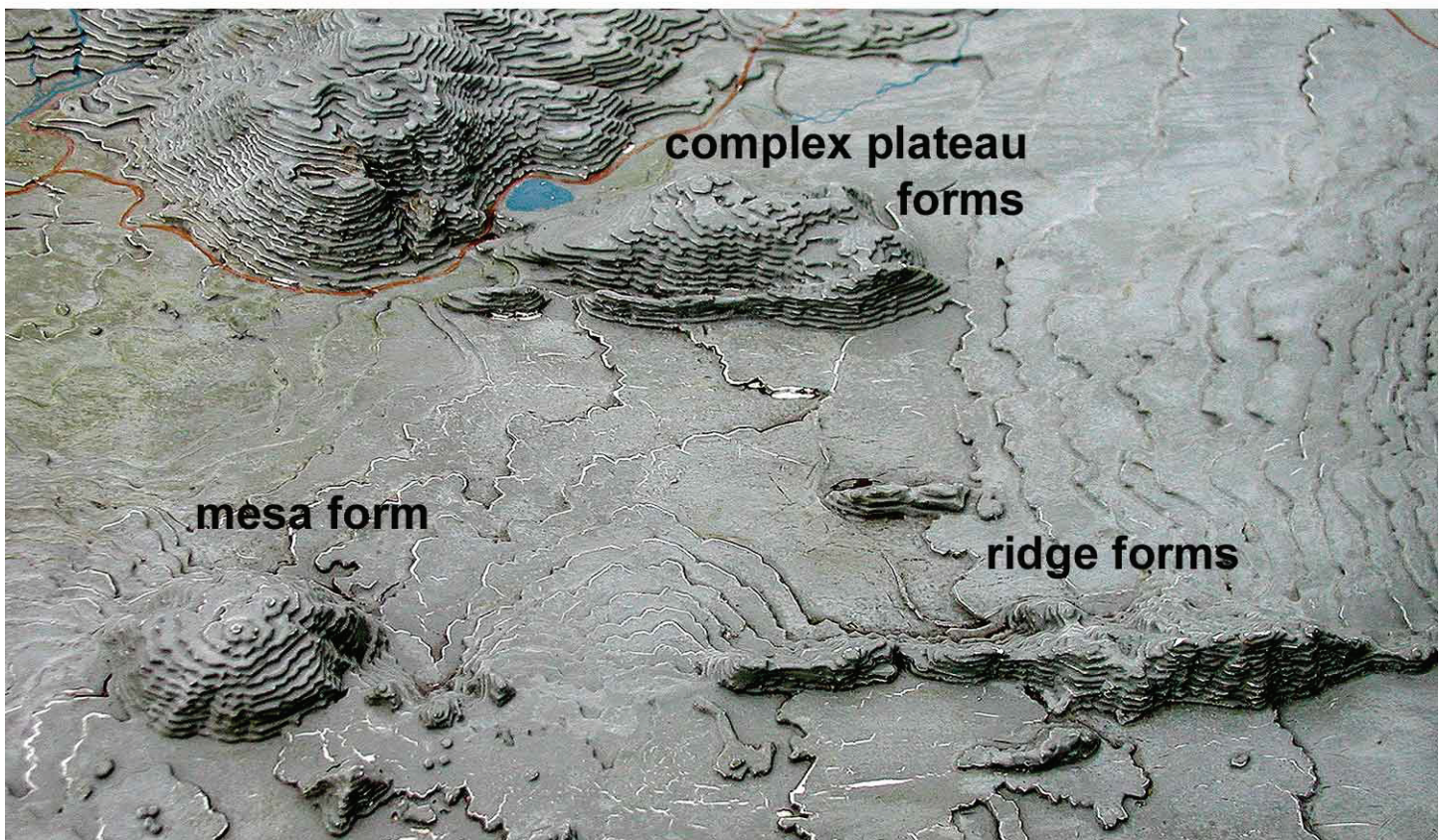
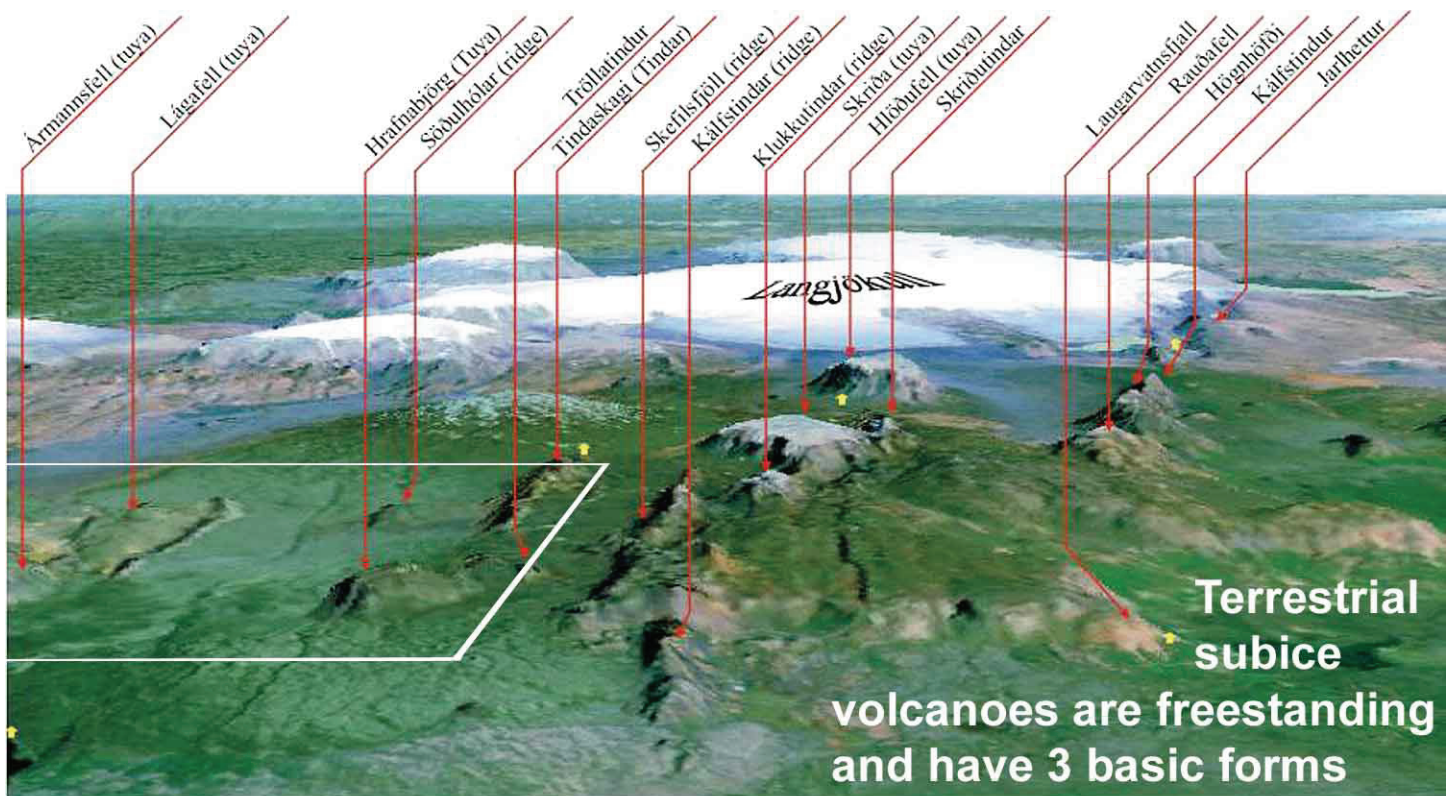


Figure 2a: Comparison of forms. Icelandic tuyas, tindars, and complex plateaus south of Langjökull ice cap, white box in top view shows location of bottom view.

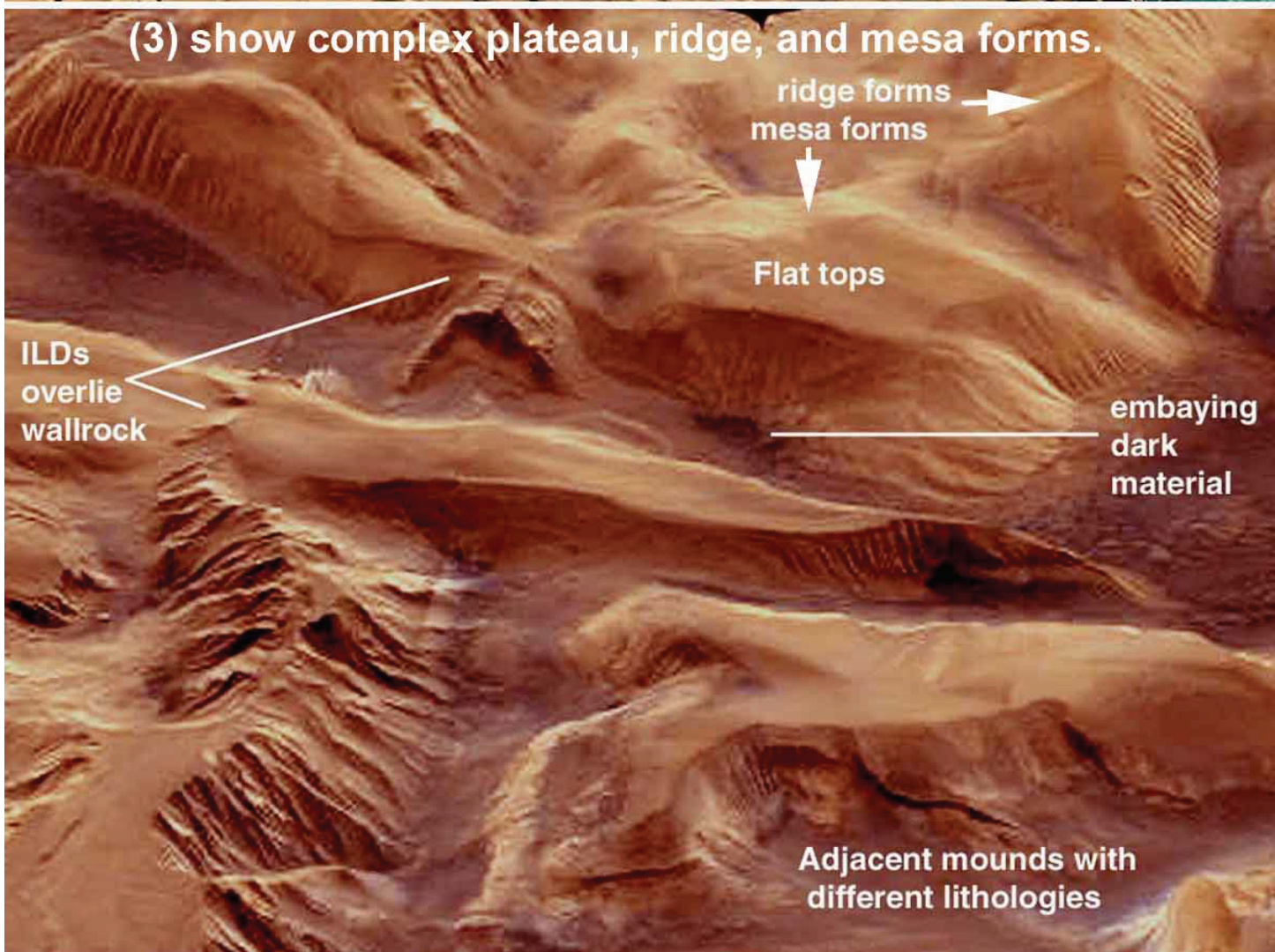
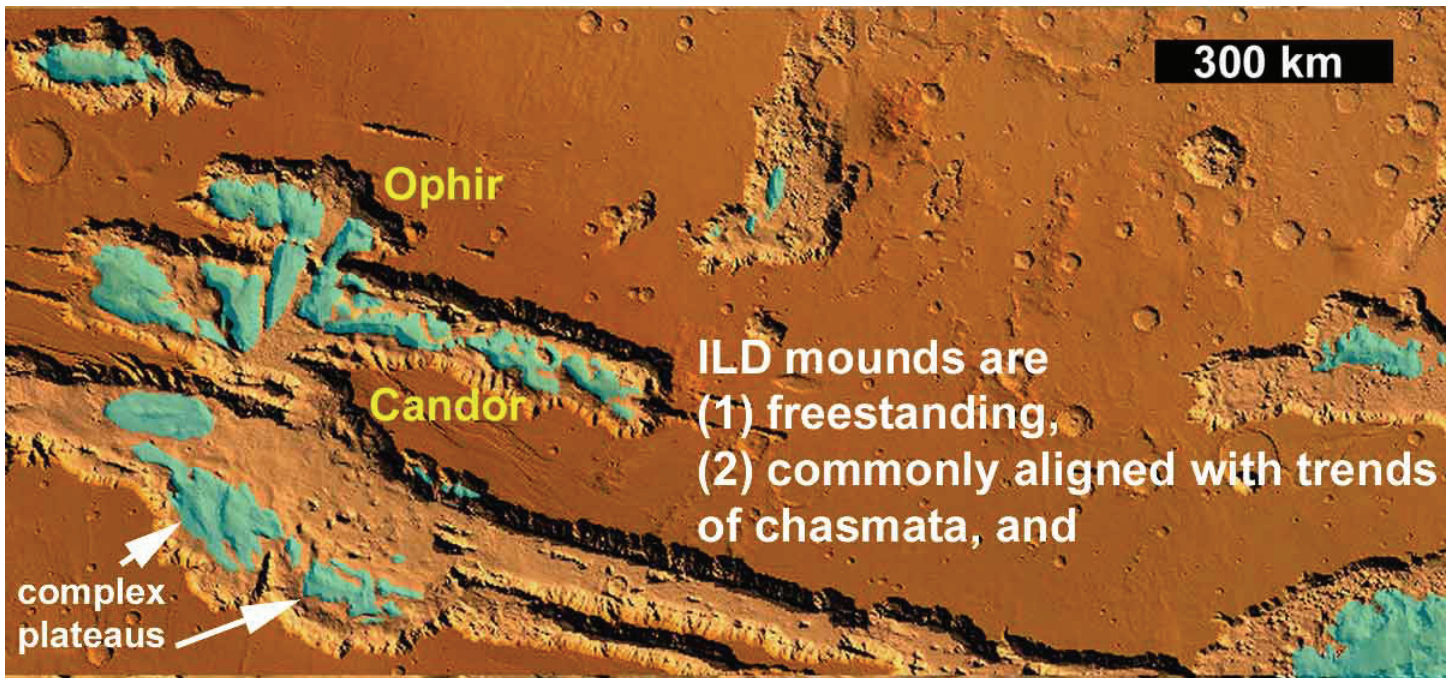


Figure 2b: Comparison of forms. Martian interior layered deposits (ILDs), bottom oblique view shows central Ophir and Candor Chasmata.

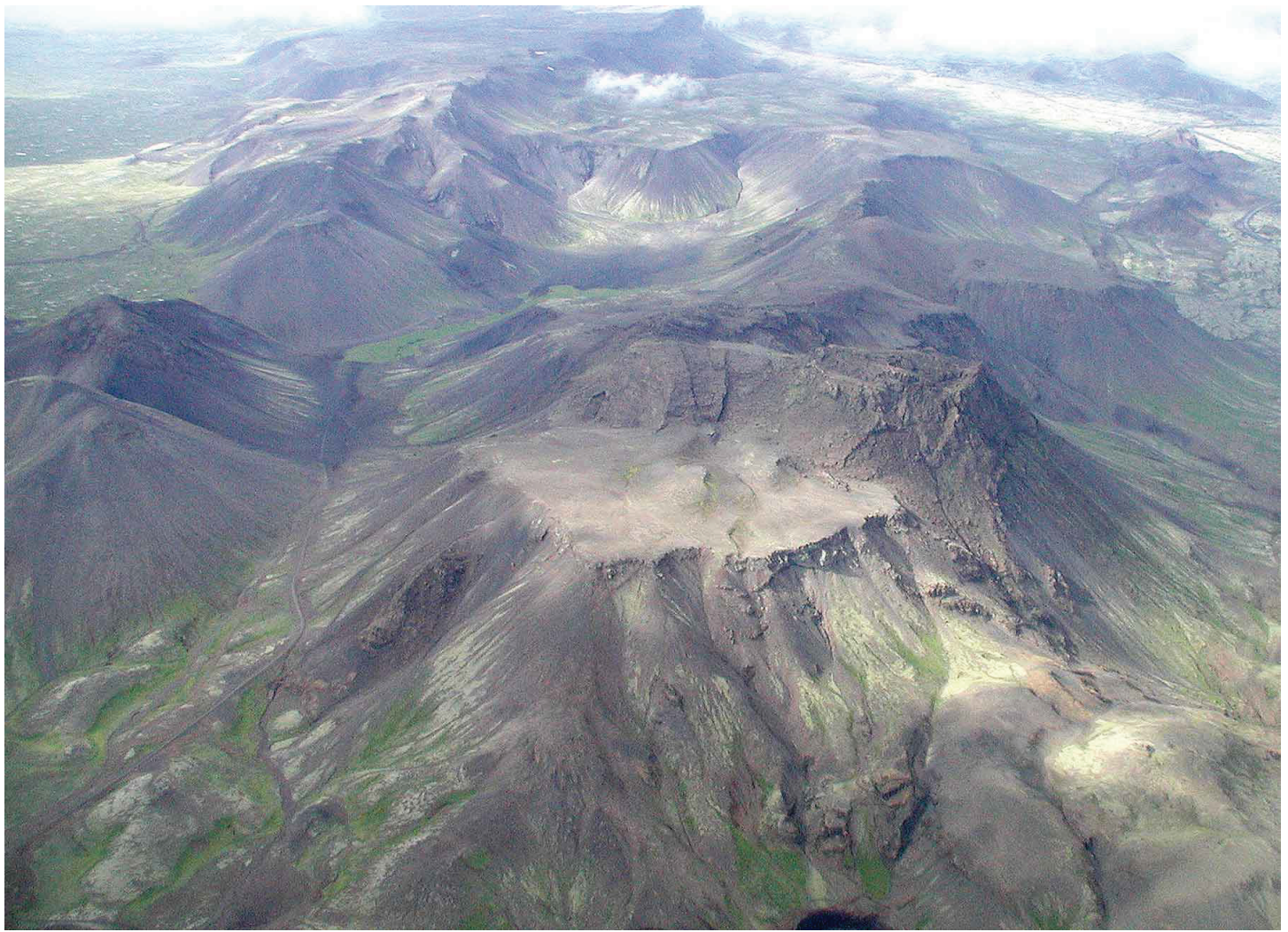


Figure 3a: Comparison of complex plateau forms. Vifilsfell, Iceland is composed of multiple overlapping subice volcanoes of differing ages.

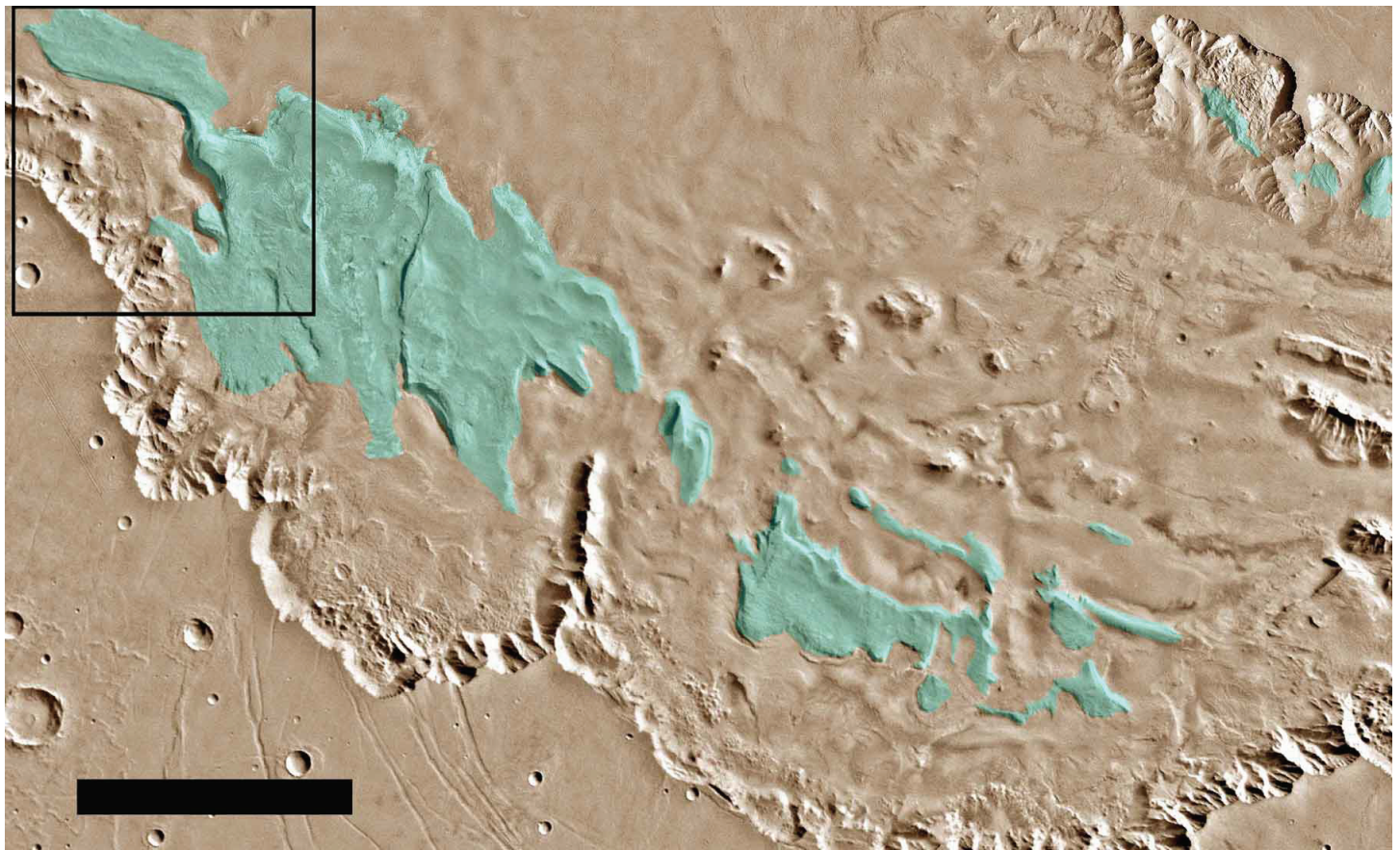


Figure 3b: Comparison of complex plateau forms. ILDs in Melas Chasma, Mars (box denote location of 17b); scale bar = 100 km (Chapman and Smellie, in submission).

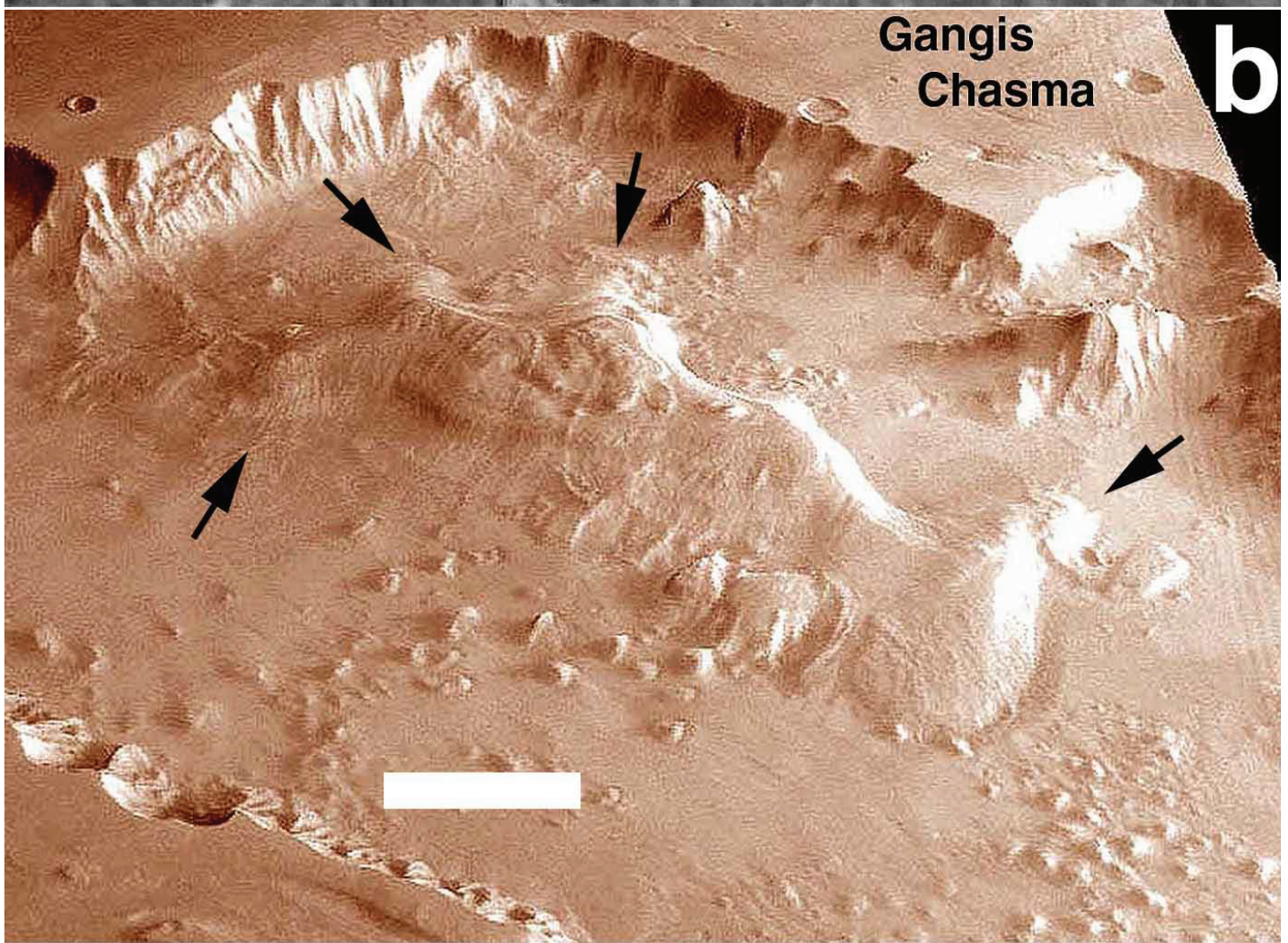
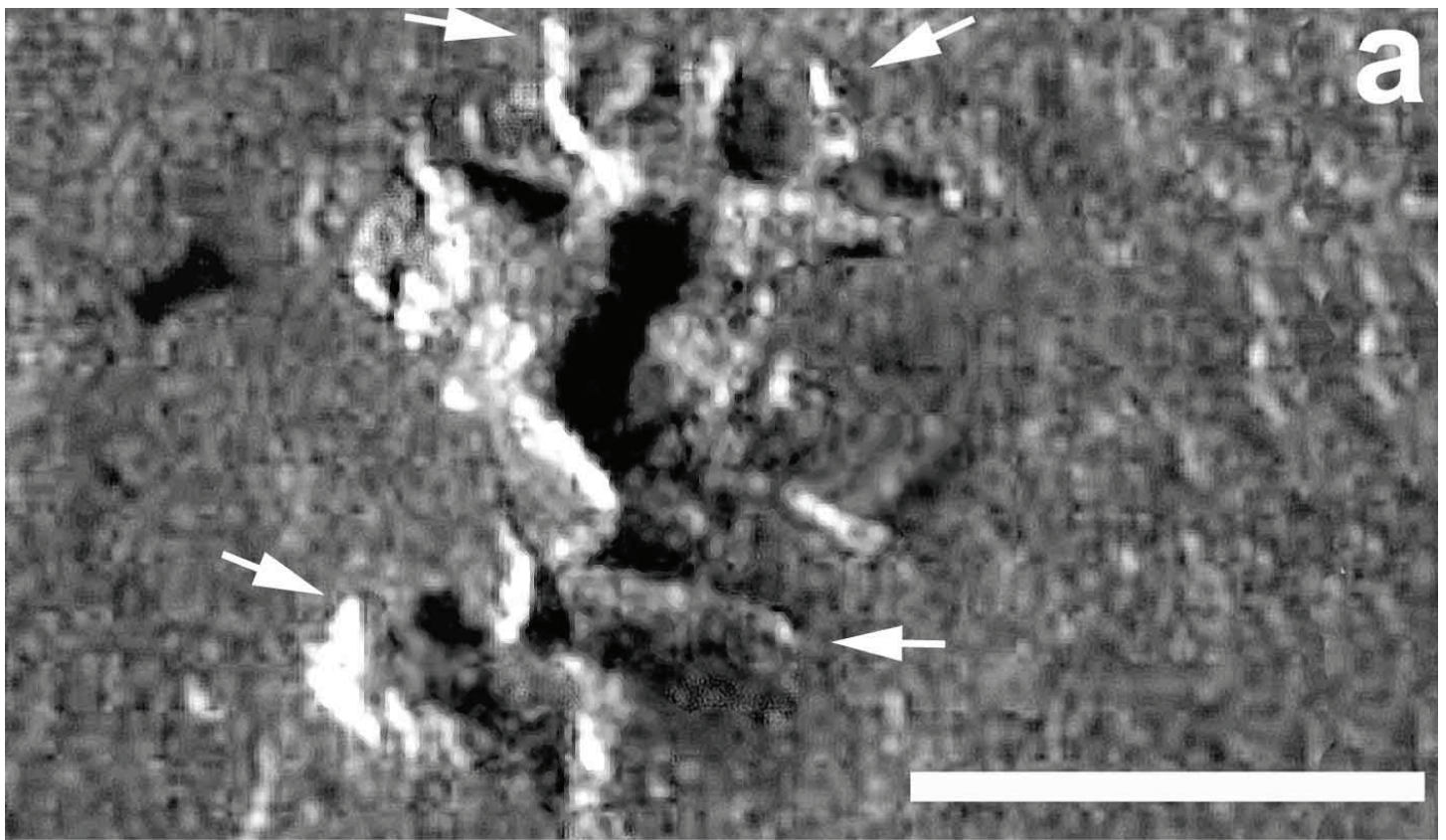


Figure 4: Comparison of cuspatate margins and wing-like flank protrusions (arrows); these protrusions are common on subice volcanoes that form beneath cold-based ice in terrestrial arctic regions. (a) Siberian Derbi-Taiga Tuya showing cuspatate margins and wing-like flank protrusions, scale bar = 5 km (part of RADARSAT image R120050130U3S016 courtesy of Goro Komatsu; Komatsu et al., 2004); (b) Viking (MDIM2) draped oblique MOLA view of Gangis Mensa, scale bar = 25 km (Chapman and Smellie, in submission; Komatsu et al., 2004).



Figure 5a & 5b: Comparison of resistant, horizontally layered caprock and steeply dipping flank materials on subice volcanoes and ILDs. (a) Tindaskagi in Iceland, boxes denote location of enlargements; (b) Mjofell Fremre, white lines indicate dip of flank beds.

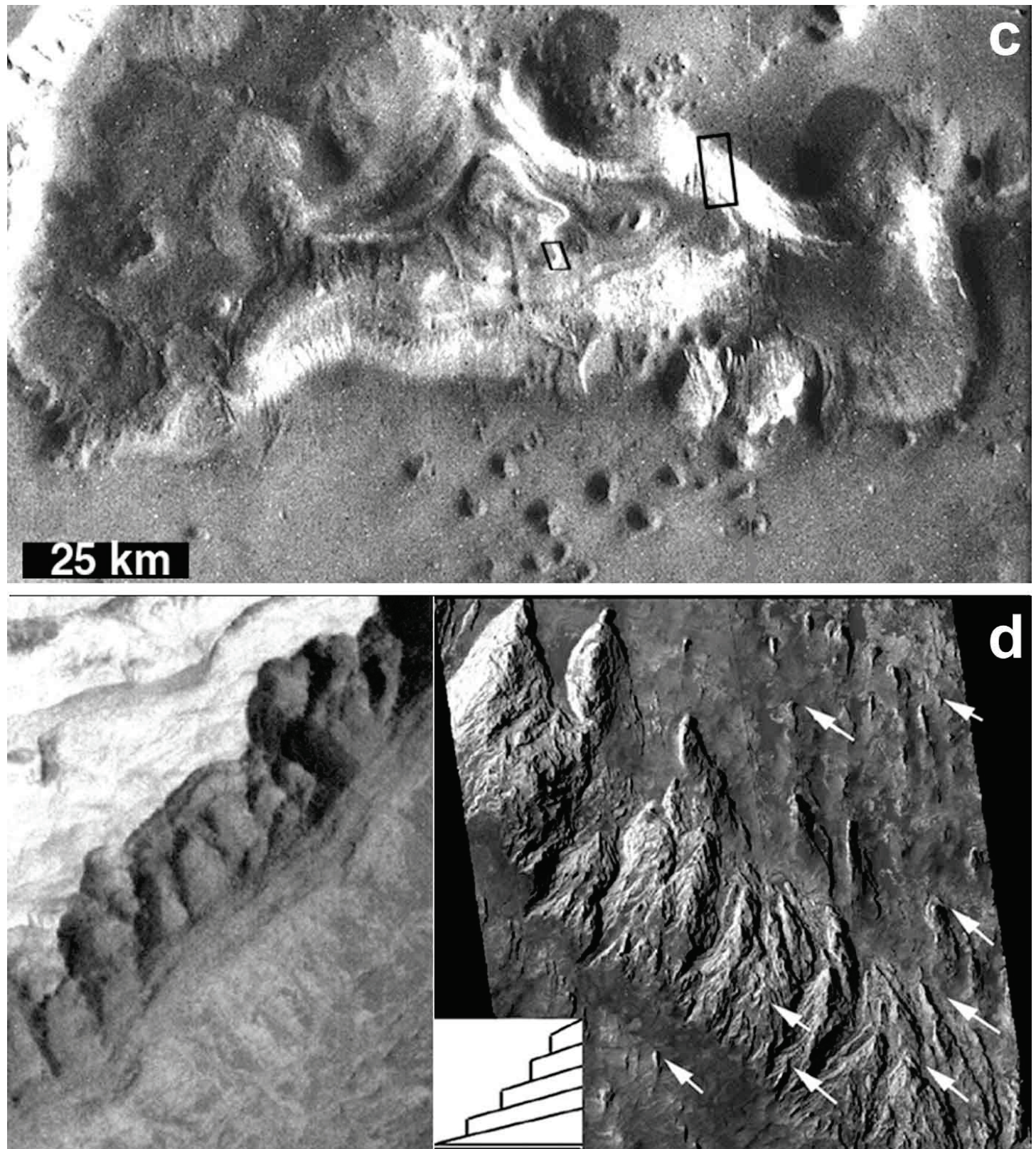


Figure 5c & 5d: Comparison of resistant, horizontally layered caprock and steeply dipping flank materials on subice volcanoes and ILDs. (c) Viking image of Gangis Mensa (boxes denote location of images on (d); (d) parts of MOC images on Gangis Mensa: on left, horizontally layered resistant caprock (M804332, 2.86 m/pixel) and on right, arrows on

flank denote alignment of ridge wedge points indicating steeply dipping layers schematically shown on illustration (M304405 and M401737 mosaic, 5.7 m/pixel).

Figure 5e: Comparison of resistant, horizontally layered caprock and steeply dipping flank materials on subice volcanoes and ILDs. Viking view of ILD ridge in central Candor Chasma (top; black box locates Viking 815A58 High Resolution (24 m/p) inset in blue), and uncapped and capped tindar ridges in Iceland (bottom).

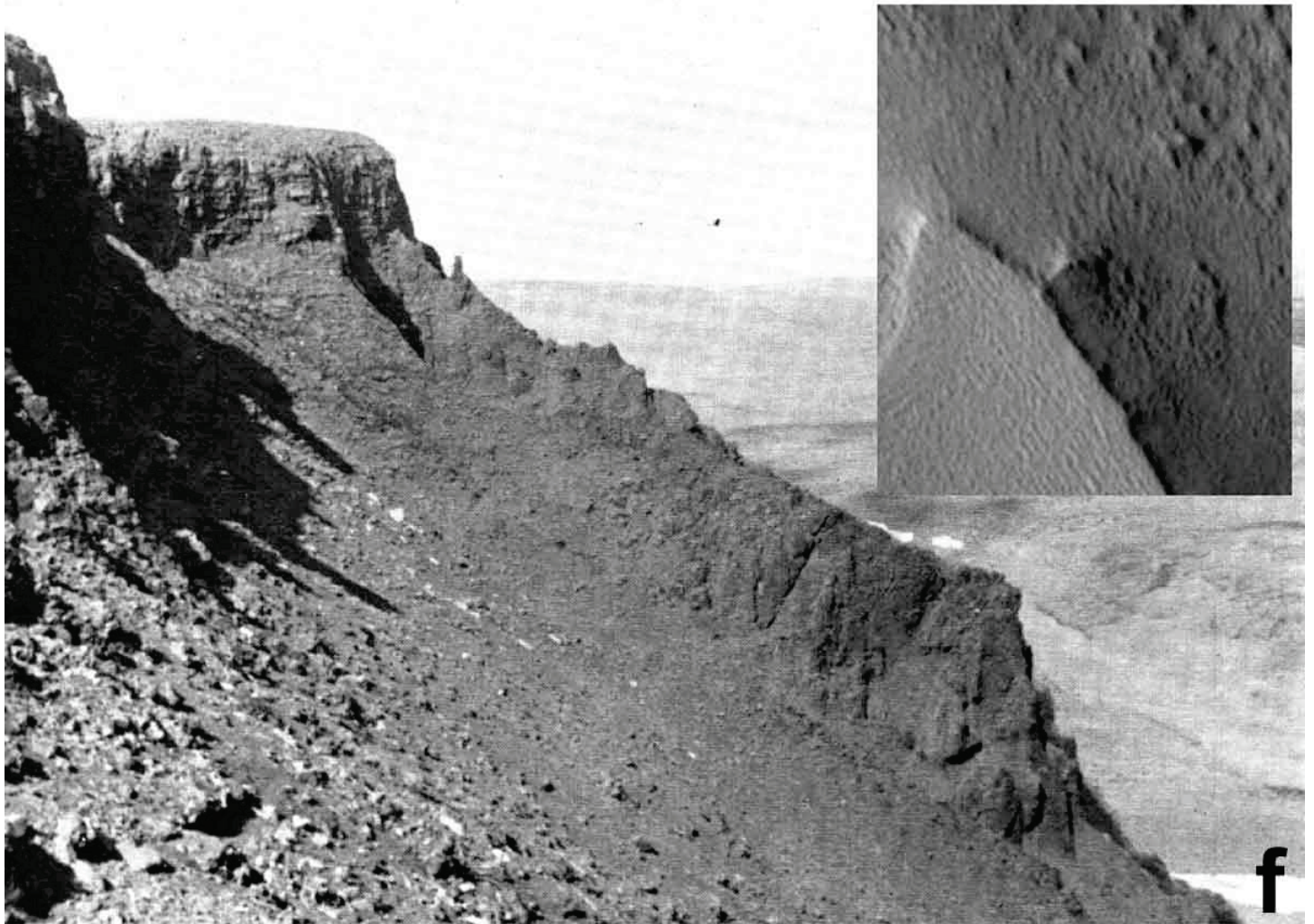


Figure 5f: Comparison of resistant, horizontally layered caprock and steeply dipping flank materials on subice volcanoes and ILDs. Eastern flank of Skeidin Tuya showing resistant lava caprock above palagonitic pillow lava breccia (adapted from Van Bemmelen and Rutten, 1955), and inset showing resistant cap of Ophir Chasma ILD on MOC 04204 (4.91 m/p; Chapman, 2002; Chapman and Tanaka, 2001).

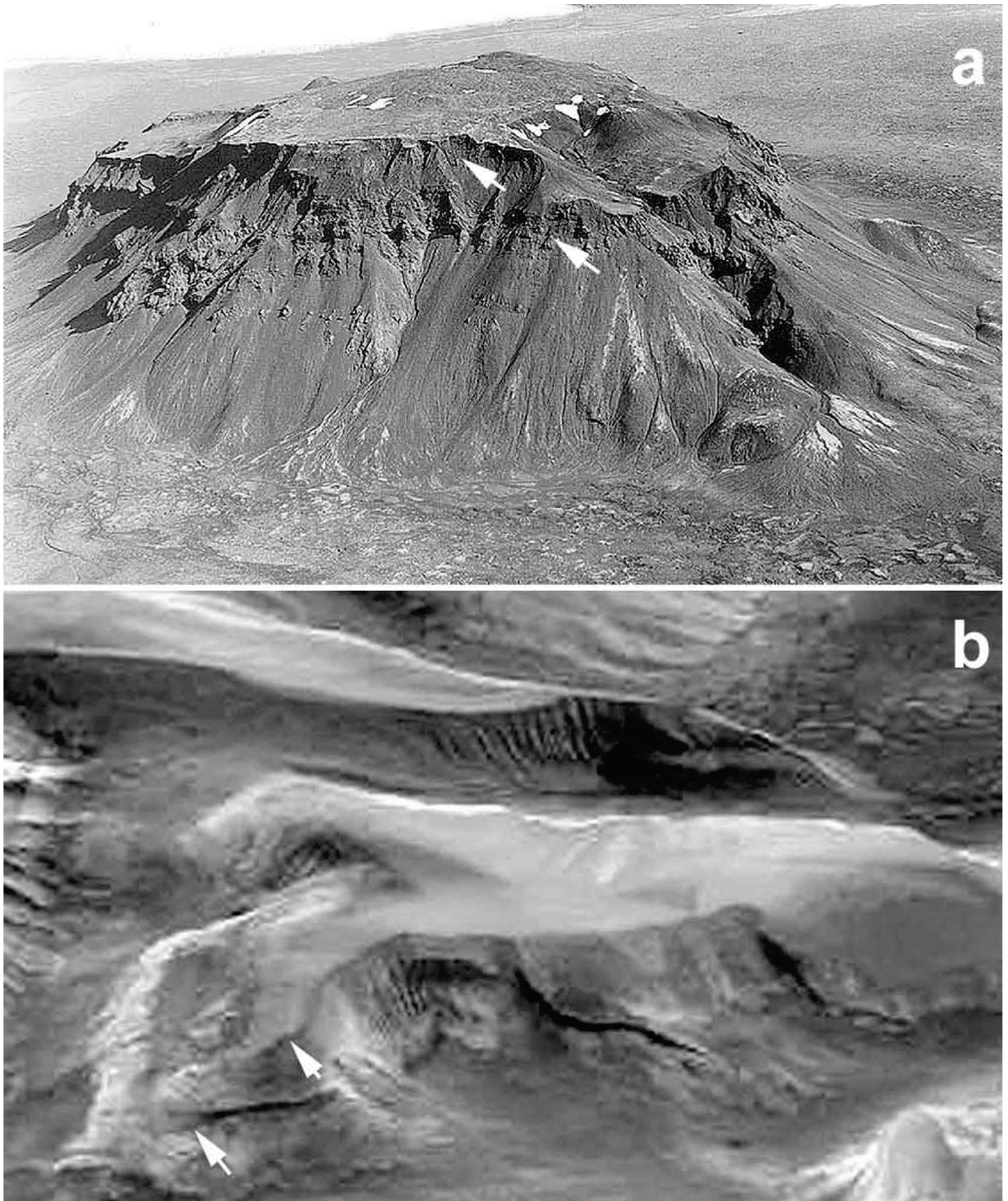


Figure 6: Comparison of double horizons of resistant caprock (arrows). (a) Icelandic Hlöðufell, sequences of horizontally layered subaerial lava, indicate 2 series of volcanic episodes that overtopped the meltwater lake (courtesy, Ian Skilling); (b) Viking draped MOLA view of Candor Mensa (110 x 50 km; Chapman and Smellie, in submission).

MOC 3-04877

5.66 m/pixel

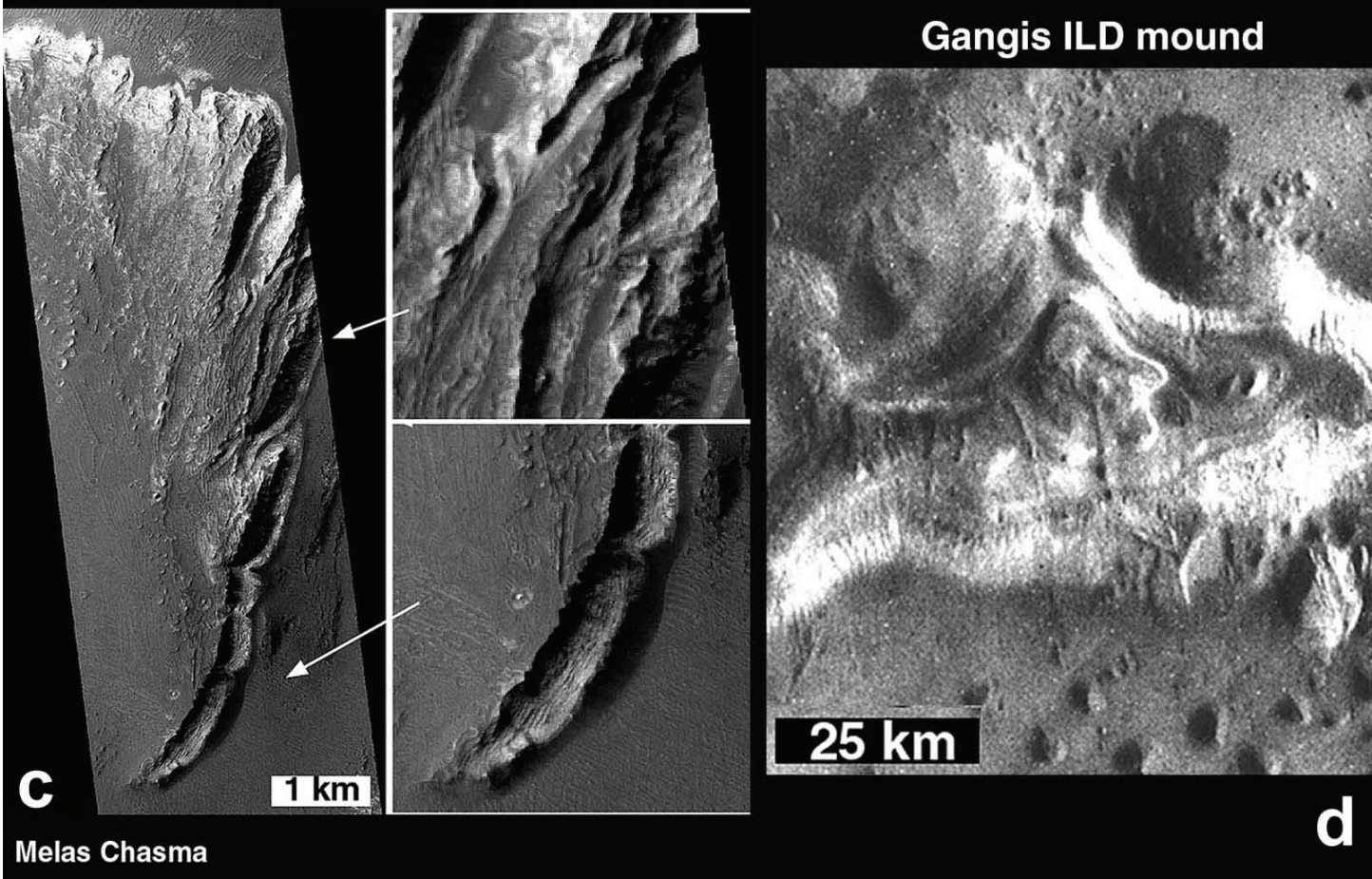


Figure 7: Comparison of resistant caprock vents on subice volcanoes and possible vents in ILDs. (a) circular volcanic crater (arrow) on 2.5 km diameter Hrafnabjörg; (b) narrow central fissure vent on 4-km-wide Herdubreidartögl (adapted from Van Bemmelen and Rutten, 1955); (c) wind-eroded pit chain in Melas Chasma ILD mesa; (d) Viking image of Gangis Mensa with narrow linear ridges on top of mound that may be vent sites (Chapman and Tanaka, 2001).

Figure 8: Comparison of possible tephra vents. (a) open-ended tephra cone in Melas Chasma ILD mesa with 2 tephra cones in northern Arizona (on top right, unnamed feature east of SP crater and ,on bottom, open-ended Sprout Crater; Chapman, 2002)); (b) New Mars Express anaglyph from Orbit 334 of Central Ophir and Candor Chasmata (3D glasses required for correct viewing) with large arrows indicating depressions and small arrows on central ridge that may be possible vent sites (image courtesy of MEX HRSC team, FU Berlin, and DLR).  
<http://berlinadmin.dlr.de/Missions/express/firsteng.shtml>



Figure 9: Ice can reform after eruptions cease and erode away evidence of vents. Comparison of nonobservable or obscure vents on: ILDs of Ophir and central Candor Chasmata (top), 2 views of the Tindaskagi subice volcano (middle), and east Lagafell subice volcano (bottom; Chapman and Smellie, in submission).

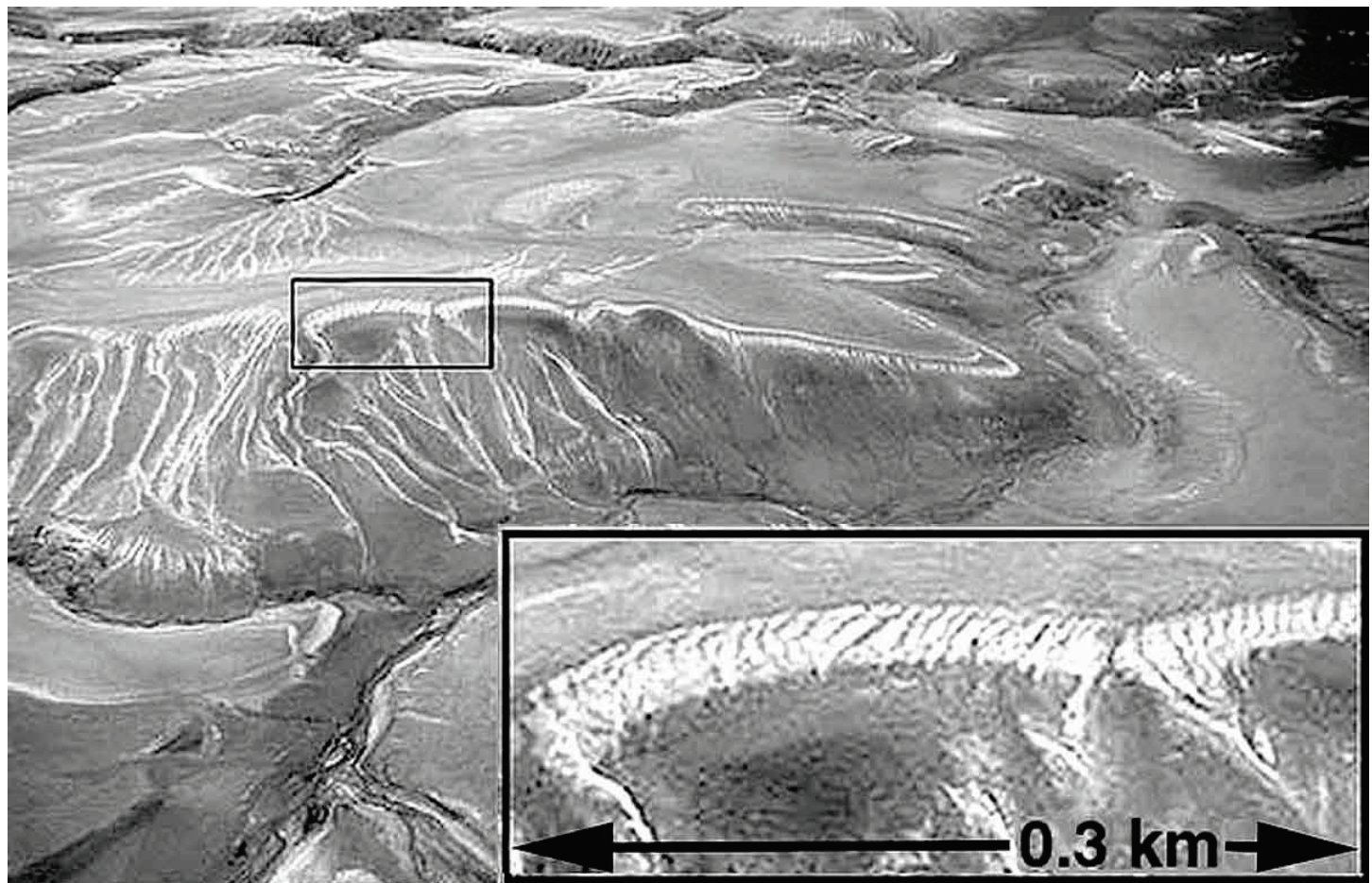


Figure 10a: Views of friable mantles on Icelandic and Martian mounds. Naefurholtsfjall Tindar is capped by Hekla ash deposits of bright white pumice and black lithics that show unusual folds and drapes (inset; Larsen and Thorarinsson, 1977).

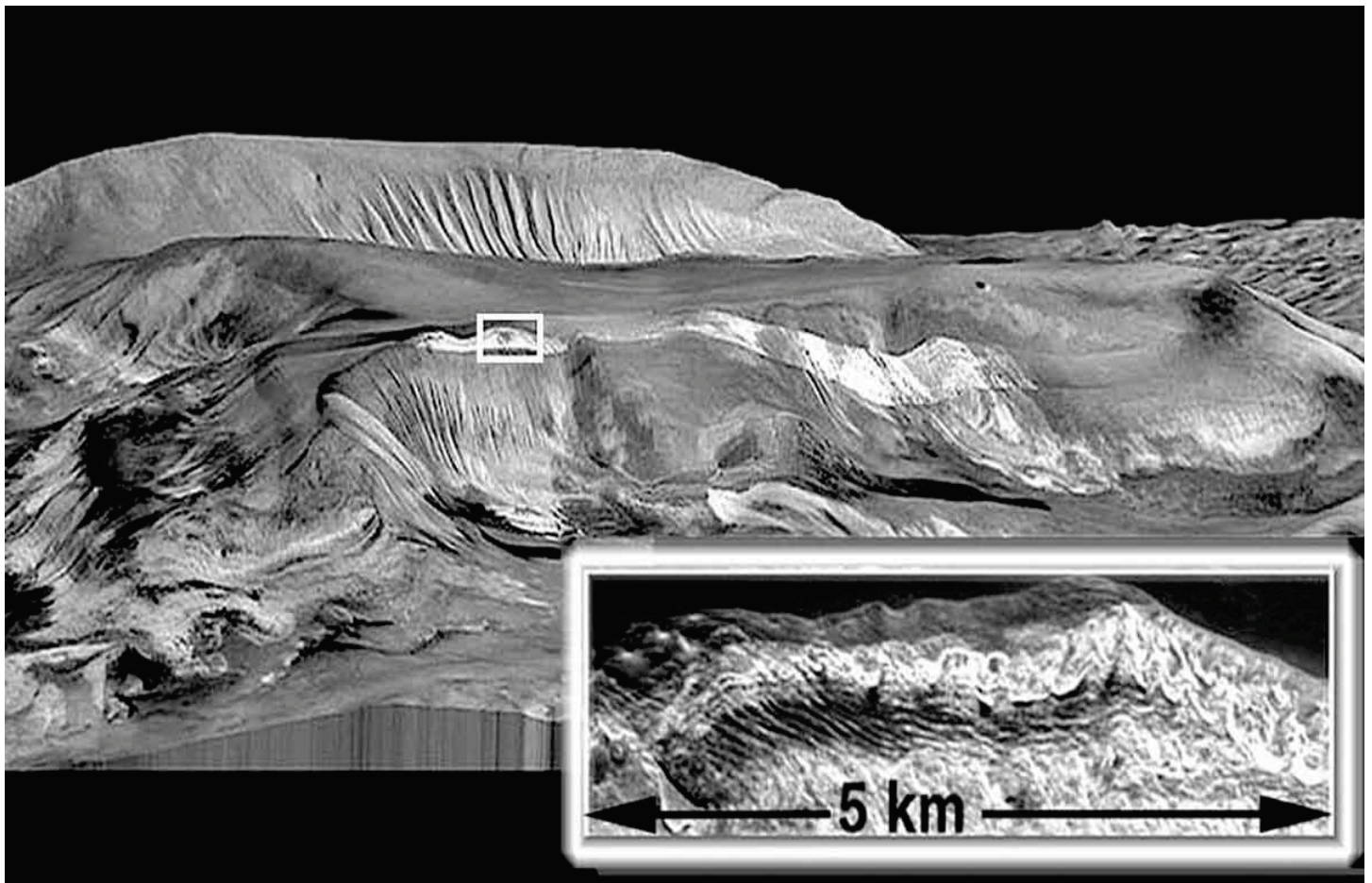


Figure 10b: Views of friable mantles on Icelandic and Martian mounds. Candor Mensa has a friable cap of mostly bright-albedo material eroded into unusual folds and drapes (inset; Chapman and Smellie, in submission).

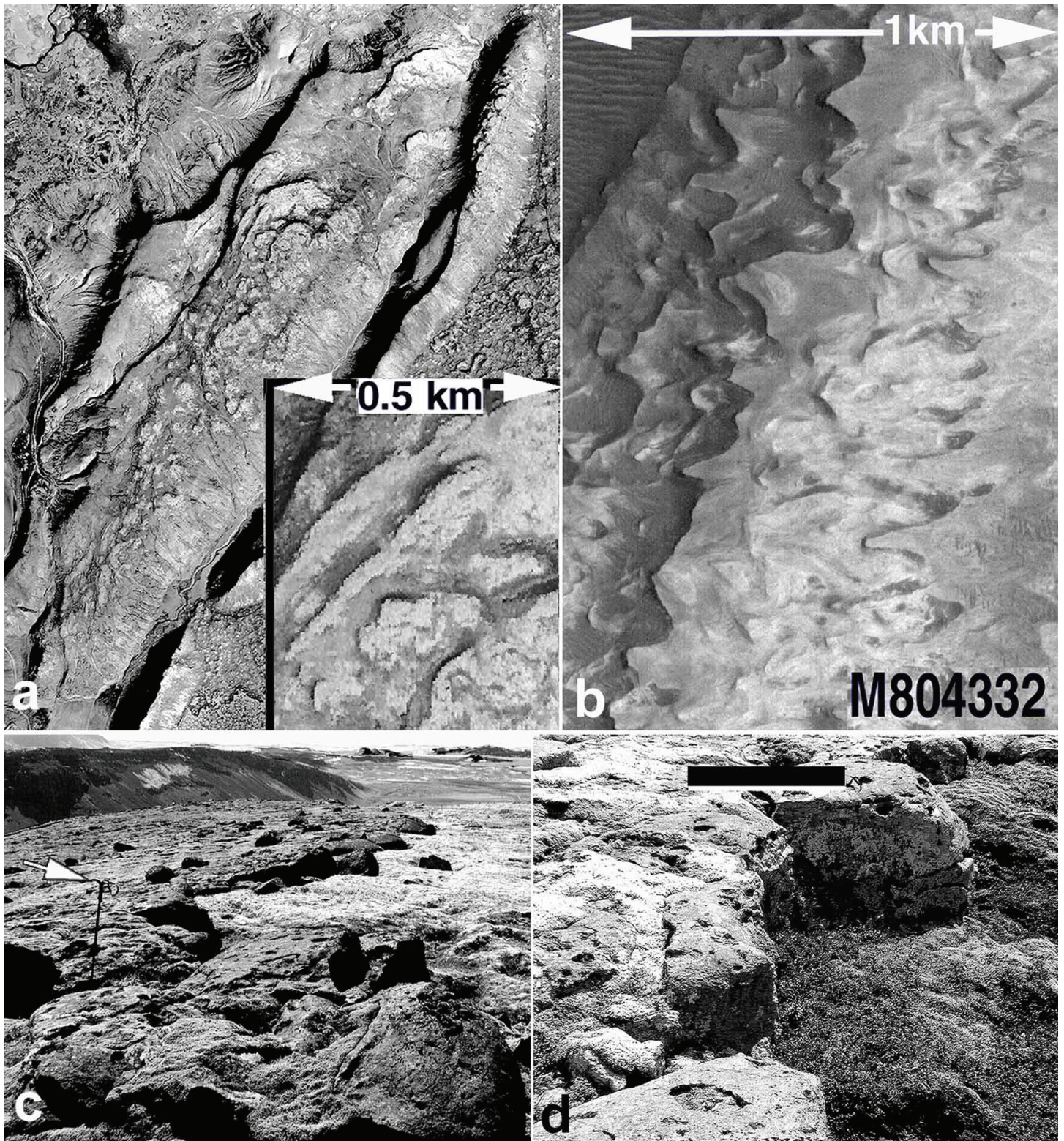


Figure 11: Resistant caprock layers with scalloped edges on Icelandic and Martian mounds. (a) Lagafell tuya; (b) MOC image of Gangis Chasma mound (rotated 180°); (c) ground view of tectonically-tilted scalloped flow on Lagafell (arrow points to top of 3 m staff); (d) note that scallops are straight edges of cooling cracks and protrusion of normal lobate weathered lava margins (3 m scale bar; Chapman and Smellie, in submission).

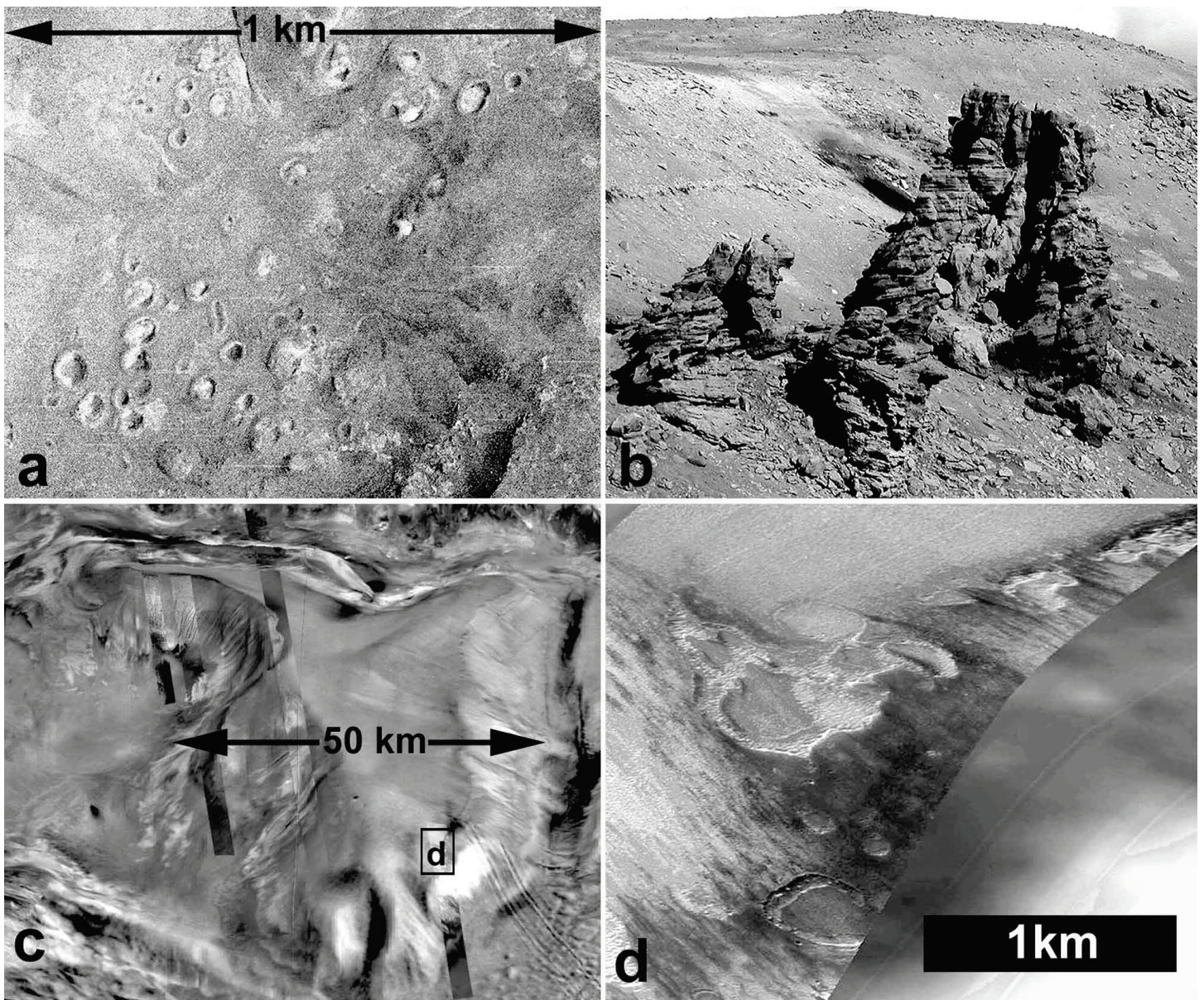


Figure 12: Pits on friable tops of Icelandic and Martian mounds. (a) maar craters on Dyngjufjöll Ytri (Sigvaldason, 1992); (b) cemented pipe-like structure that mark the subsurface center of a now eroded maar crater on east side of Dyngjufjöll Ytri; (c) Viking and MOC draped MOLA view of Candor Mensa (box indicates location of d); (d) irregularly shaped, mostly filled pits on part of MOC image M1300507 (5.81 m/pixel; Chapman and Smellie, in submission).



Figure 13: Nearly horizontal, fine to massive layers in: (a) part of MOC image M1801893 (5.83 m/pixel) on west midpoint of Candor Mensa, and (b) approximately 1-km-wide aerial view of Tindaskagi; (c) approximately 1-km-wide

aerial view of variably dipping, fine to massive layers within Skrida Tindar; individual layers on subice volcanoes are due to repeated volcanic eruptions that generate huge columns of material into the air that fall back into the meltwater lake to settle on the horizontal areas and to cascade down steep volcanic slopes; thickness is determined by the volume of each eruption; degree of bed horizontality depends of the topography of the underlying edifice (Chapman and Smellie, in submission).

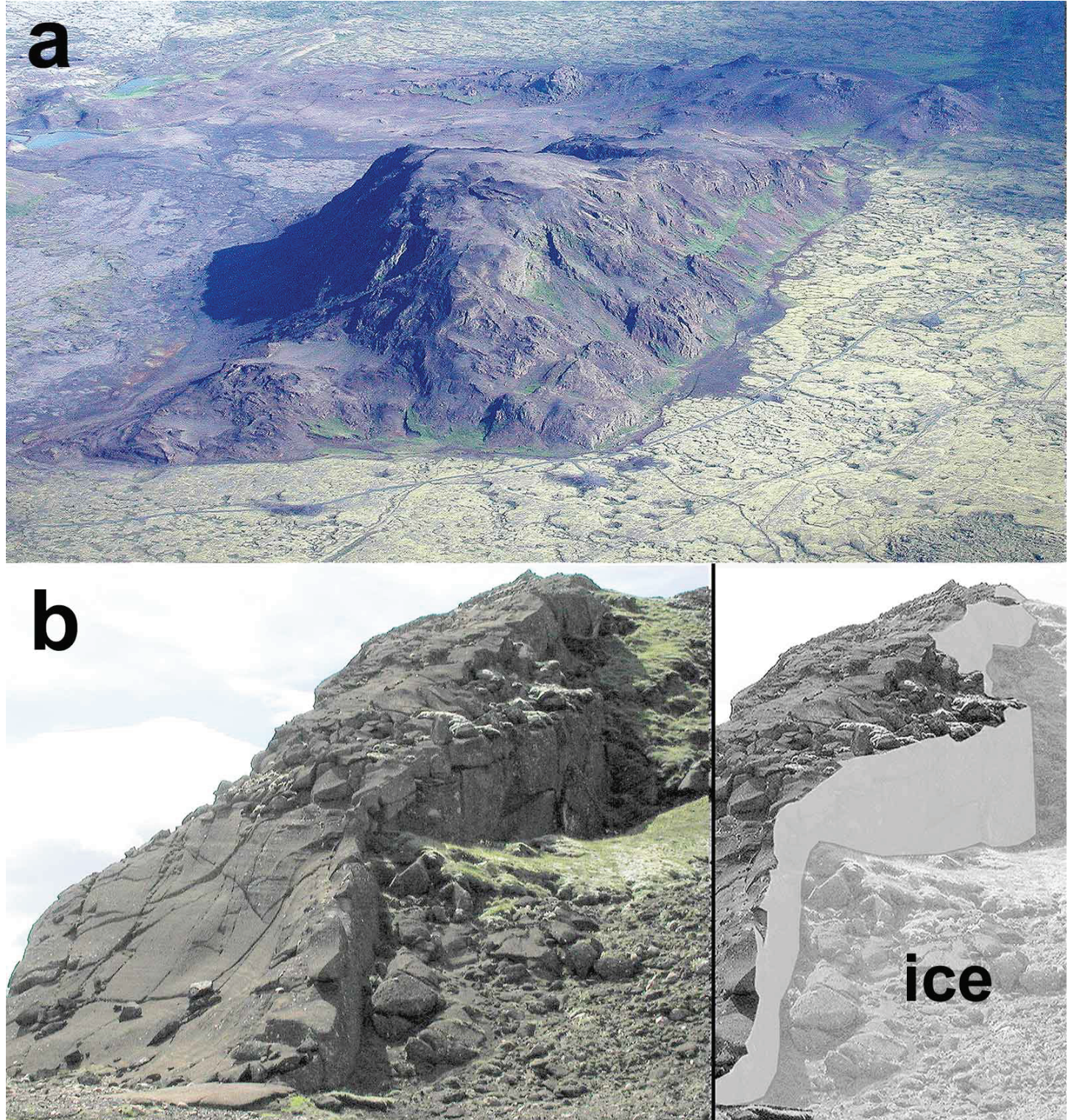


Figure 14a & 14b: Abrupt flank terminations of sub-ice volcanoes and ILDs. (a,b) Views of 900-m-wide Helgafell Tindar in Iceland; (a) aerial image shows very linear, abrupt east flank termination formed because hyaloclastic material was

dammed against a coeval ice sheet that has since melted away (Schopka et al., 2003); (b) left, view of north Helgafell showing tephra flow lobe with a steep west wall, and right, gray shading marking possible location of a former ice wedge.

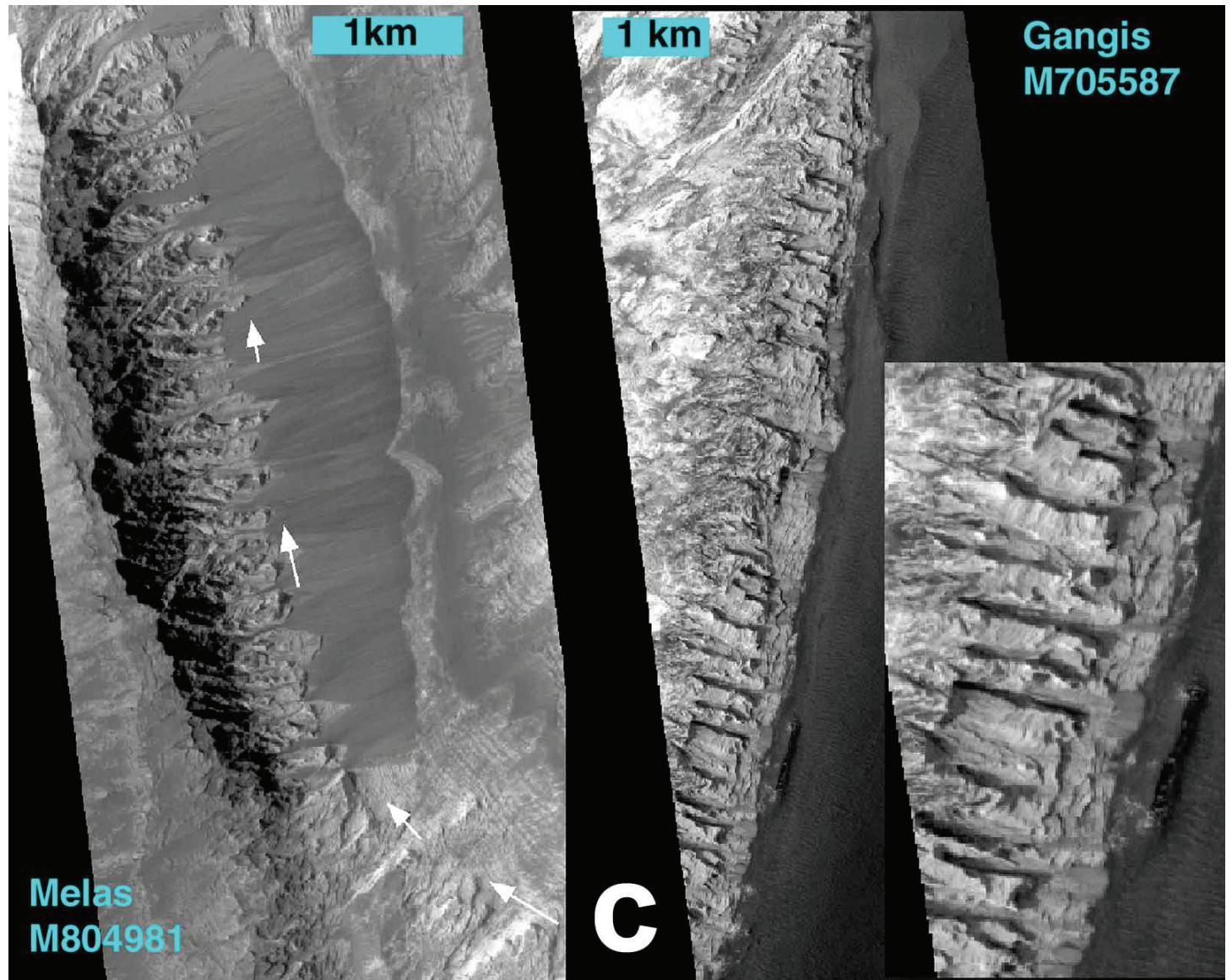


Figure 14c: Views of Melas and Gangis Chasmata ILD mounds showing abrupt flank terminations.

Figure 14d: Part of Mars Express Anaglyph Orbit 334 (courtesy of MEX HRSC team, FU Berlin, and DLR; 3D glasses required) showing central Candor Chasma with white arrows indicating 2 levels of floor material dams, black arrows indicated grooves cut into pre-existing ILDs (see enlargement in e), and stars (enlargement in f) denoting abrupt flank termination of ILD (presumably a floor glacier dammed coeval material and cut grooves into pre-existing deposits).

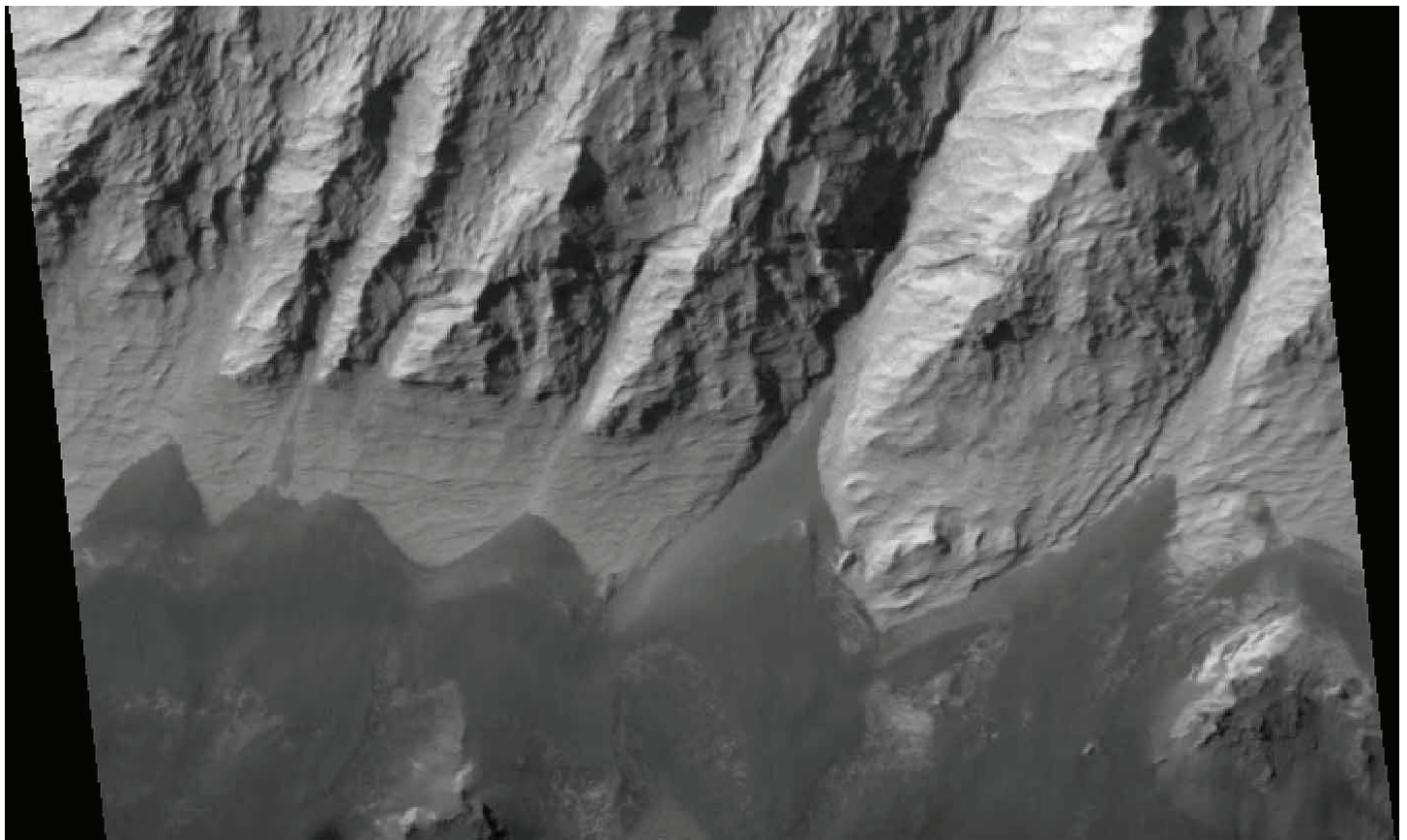


Figure 14e: Part of MOC image E1900200 (2.87 km wide; courtesy Malin Space Science Systems) showing sheared off ILD cliffs (left black arrow on d).

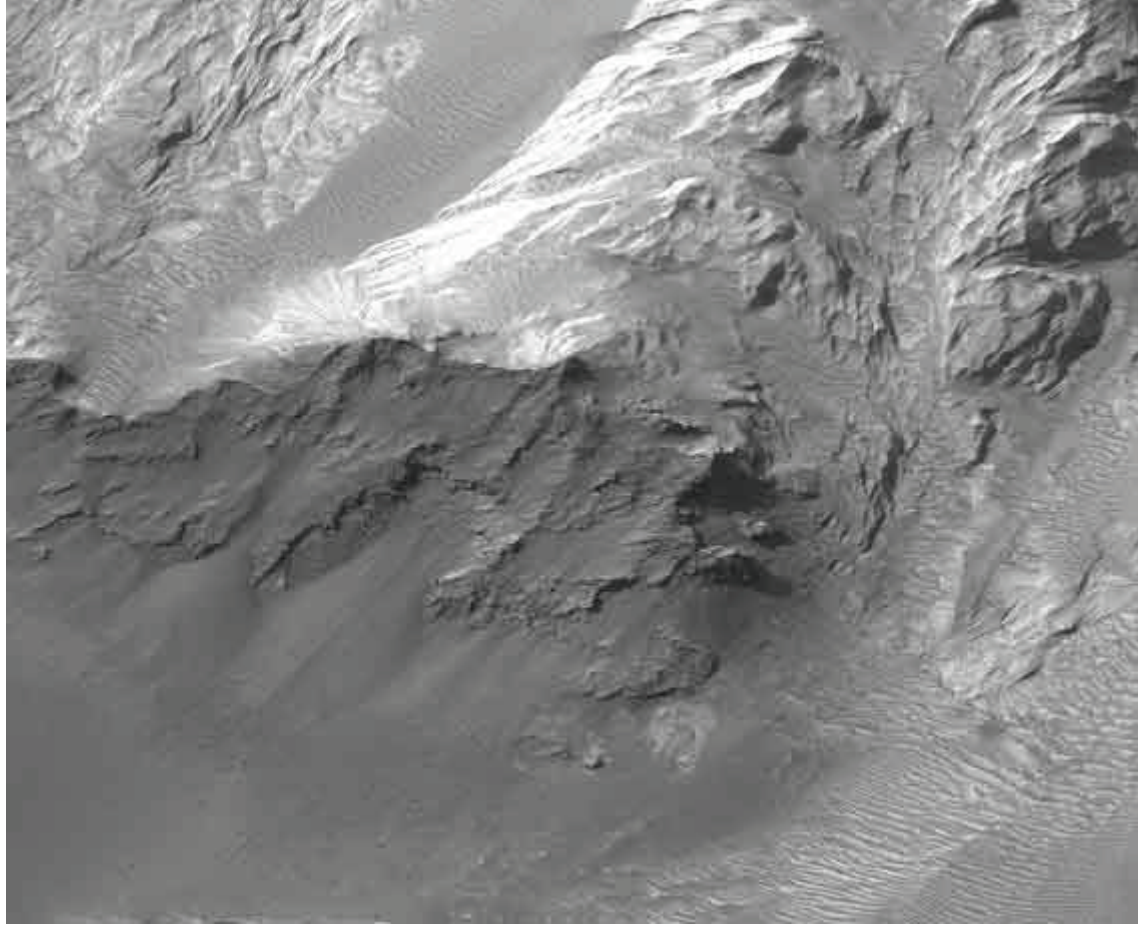


Figure 14f: Part of MOC image E101343 (1.5 km wide; courtesy Malin Space Science Systems) showing abrupt termination of ILD (star locale on d). <http://berlinadmin.dlr.de/Missions/express/firsteng.shtml>

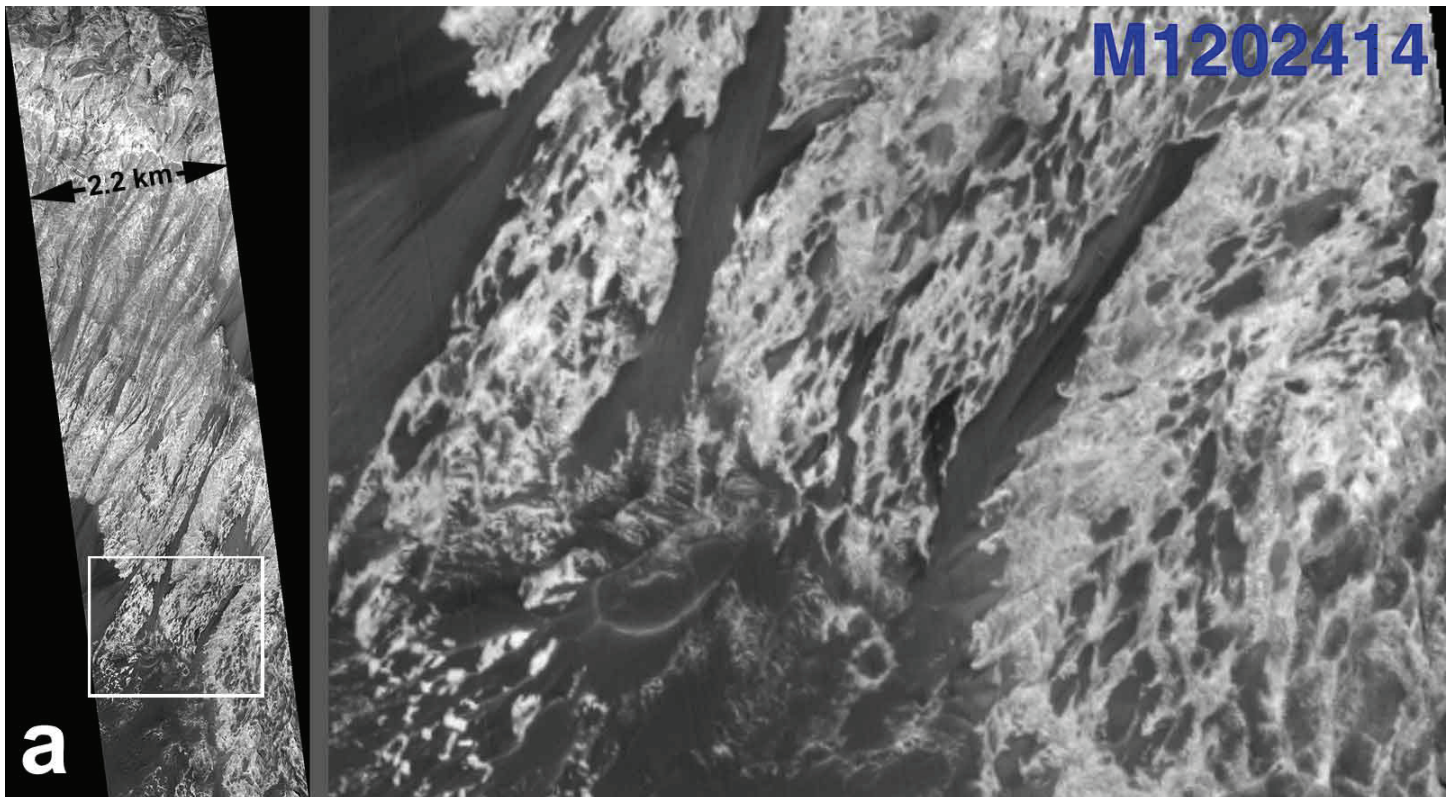
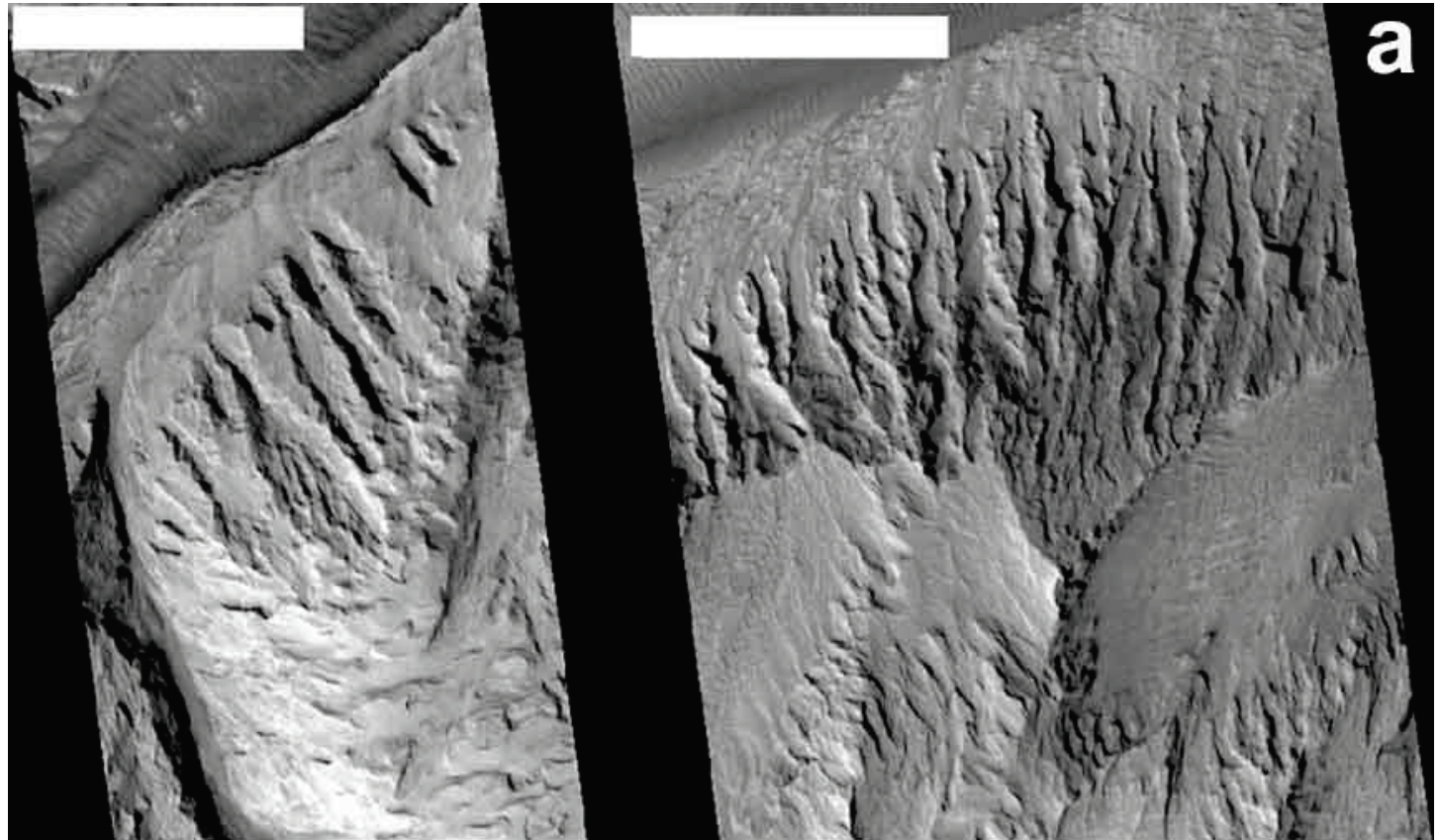




Figure 15: Images showing lack of boulders at MOC resolution. (a) MOC image M1202414 (2.2 km wide; courtesy Malin Space Science Systems) of Hebes Chasma ILD flank showing no observable boulders; (b, c, d) Views of 2 types of

armoring on Icelandic tindars: (b) boulderless slope of Armansfell (15-m-wide road on lower right for scale) is a result of armoring due to cohesive (lacking internal cooling cracks or joints) and cemented fluvio-glacial and hyaloclastic tuff that were deposited at the angle of repose; (c) south end of Naefurholtsfjall (arrow points to location of d) is armored by a veneer of pebbles to fist-size cobbles of rounded volcanic lavas (camera case and hammer for scale in right foreground); (d) Naefurholtsfjöll fluvio-glacial deposits, consisting of angled and horizontal beds of rounded lava clasts embedded in a matrix of hyaloclastic ash that weathers away leaving behind an inclined pediment armor of rounded rocks on the flanks of the edifice (Chapman and Smellie, in submission).



a



b

Figure 16: Gullies cut into discreet, low lying flanks on Martian and Icelandic mounds. (a) MOC images M1003480 on left and M1102514 on right (scale bars = 1 km) of ILDs in east Candor Chasma, these types of gullies are eroded into all sides of the ILDs including their north-facing slopes (therefore solar heating alone did not generate the gullies, but rather some internal heating mechanism); (b) Naefurholtsfjöll tindar showing Hekla in background and gullies cut into discreet layers due to infiltration of precipitation that breaks out of slopes when it encounters less permeable horizons.

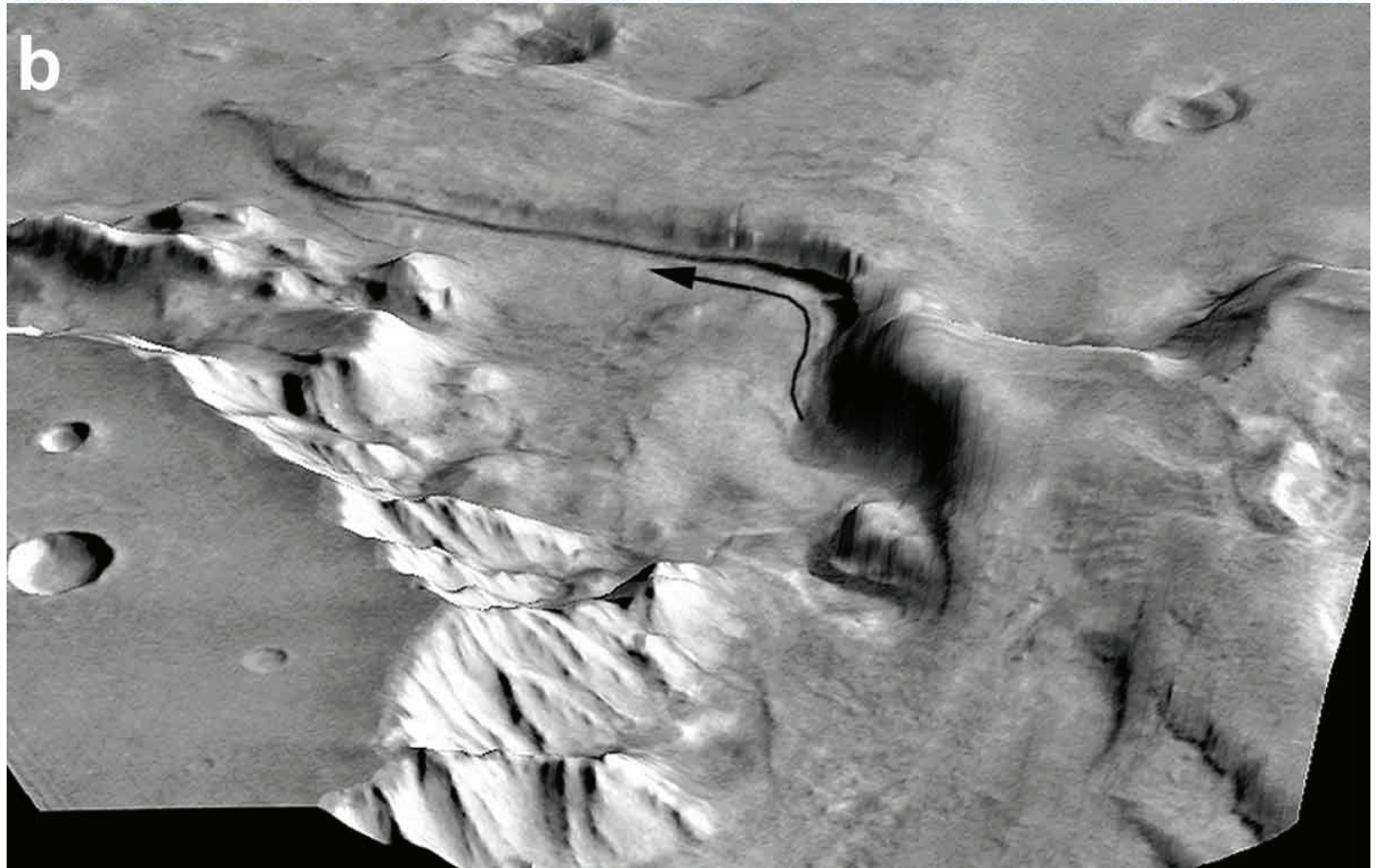
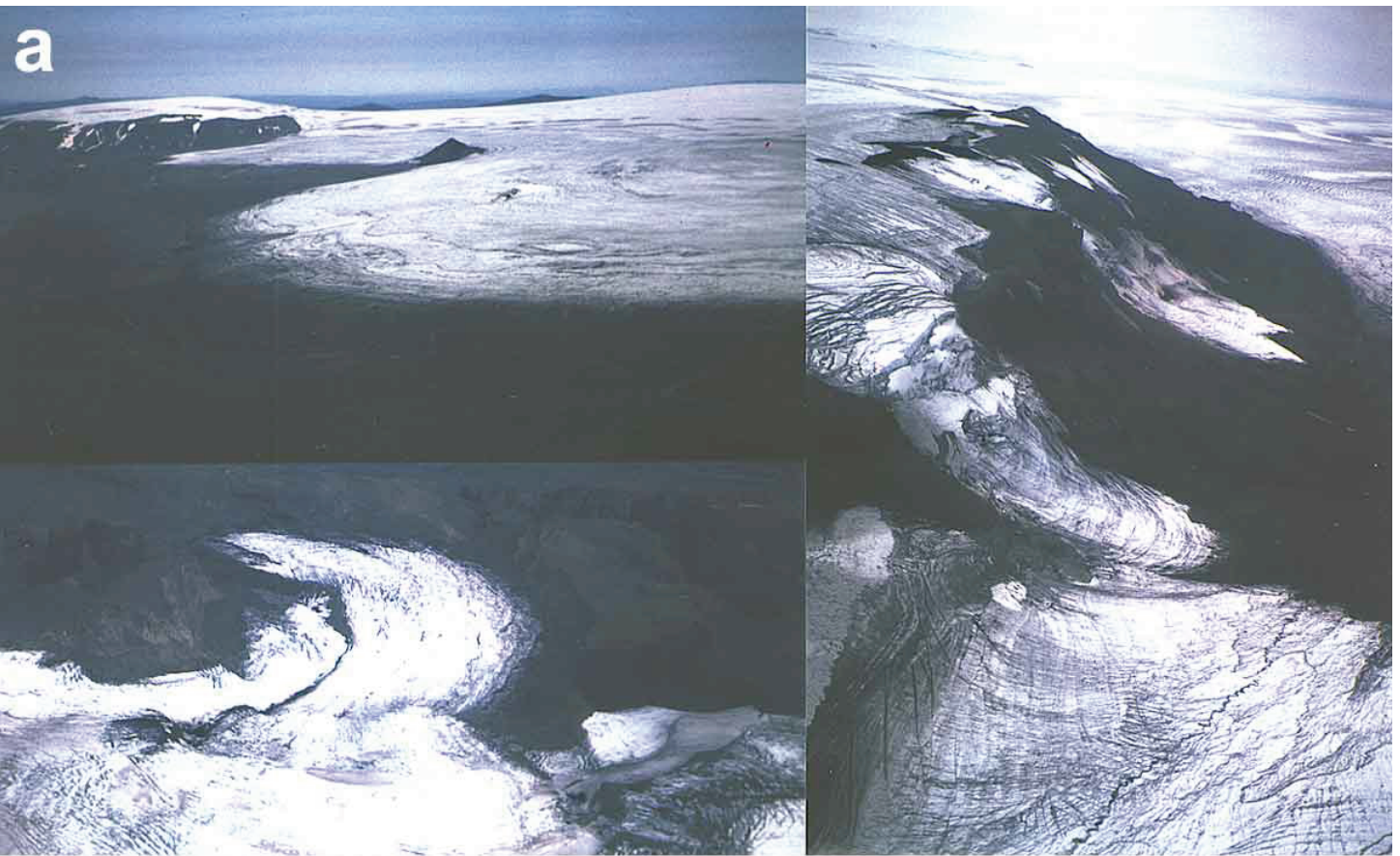


Figure 17a & 17b: Unusual canyons and hollows. (a) after an eruption ceases ice caps can reform and cover volcanoes and their glaciers can carve canyons like these shown on Icelandic subice volcanoes; (b) Cirque-shaped head and u-shaped flat-floored canyon with sharp angled curve (arrow) cut into west Melas ILD (location on 3b).



C



d

Figure 17c & 17d: Unusual canyons and hollows. (c) chains of glacial cirques in Icelandic mountains; (d) chains of cirque-like hollows in ILDs of east Candor Chasma.

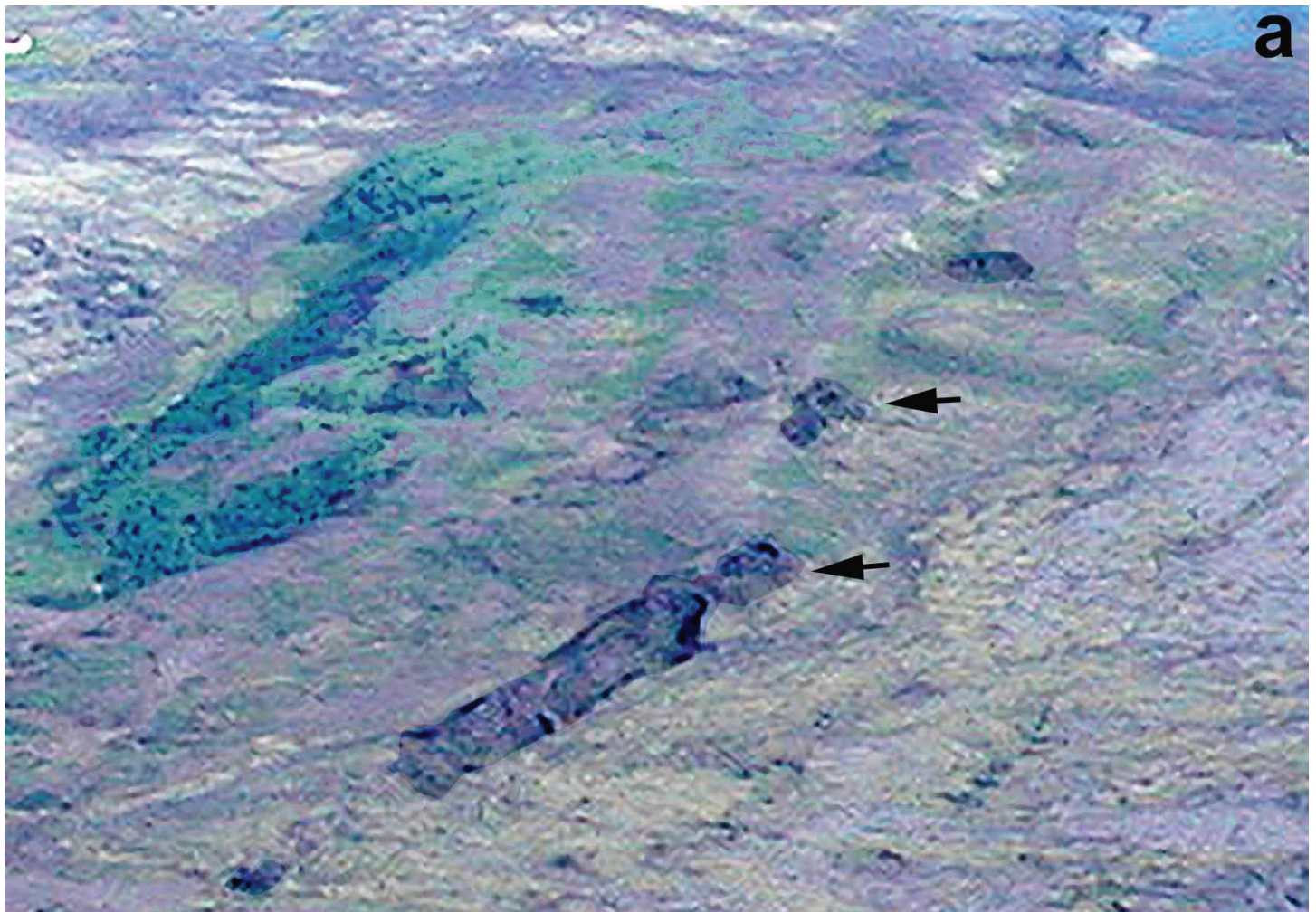


Figure 18a & 18b: As expected in a volcanically active area, young volcanoes can intrude older volcanic deposits. (a) Sub-ice Undirhlíðar pillow lava mound in Iceland intruded by younger subaerial cinder cones (arrows mark arrowed features in b); (b) Ground view of Undirhlíðar.

**MOC**  
**M1000466**  
**2.86 m/p**

← 1 km →

**C**

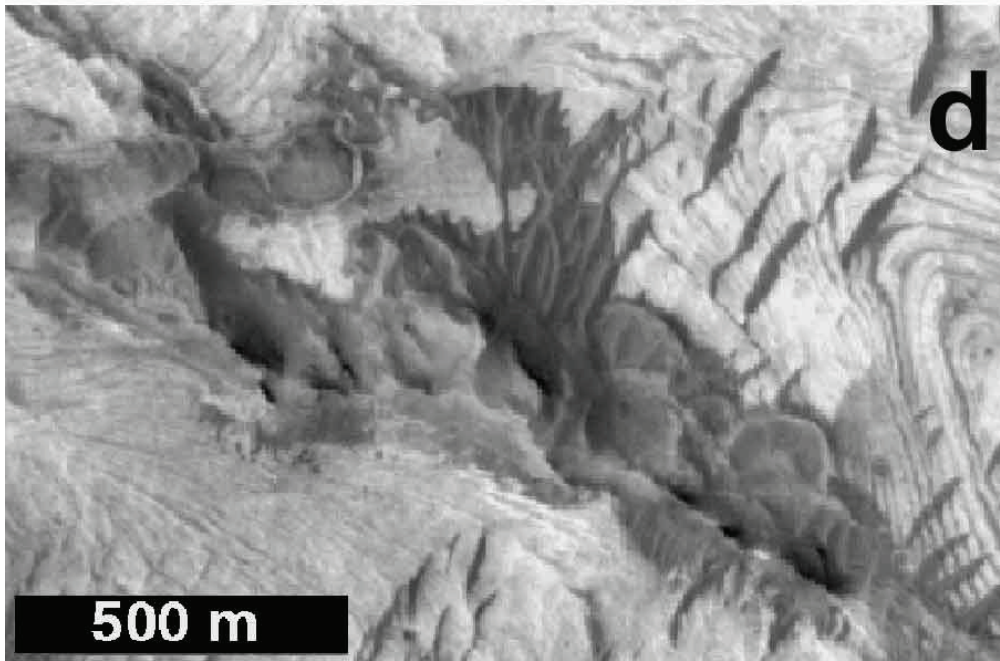
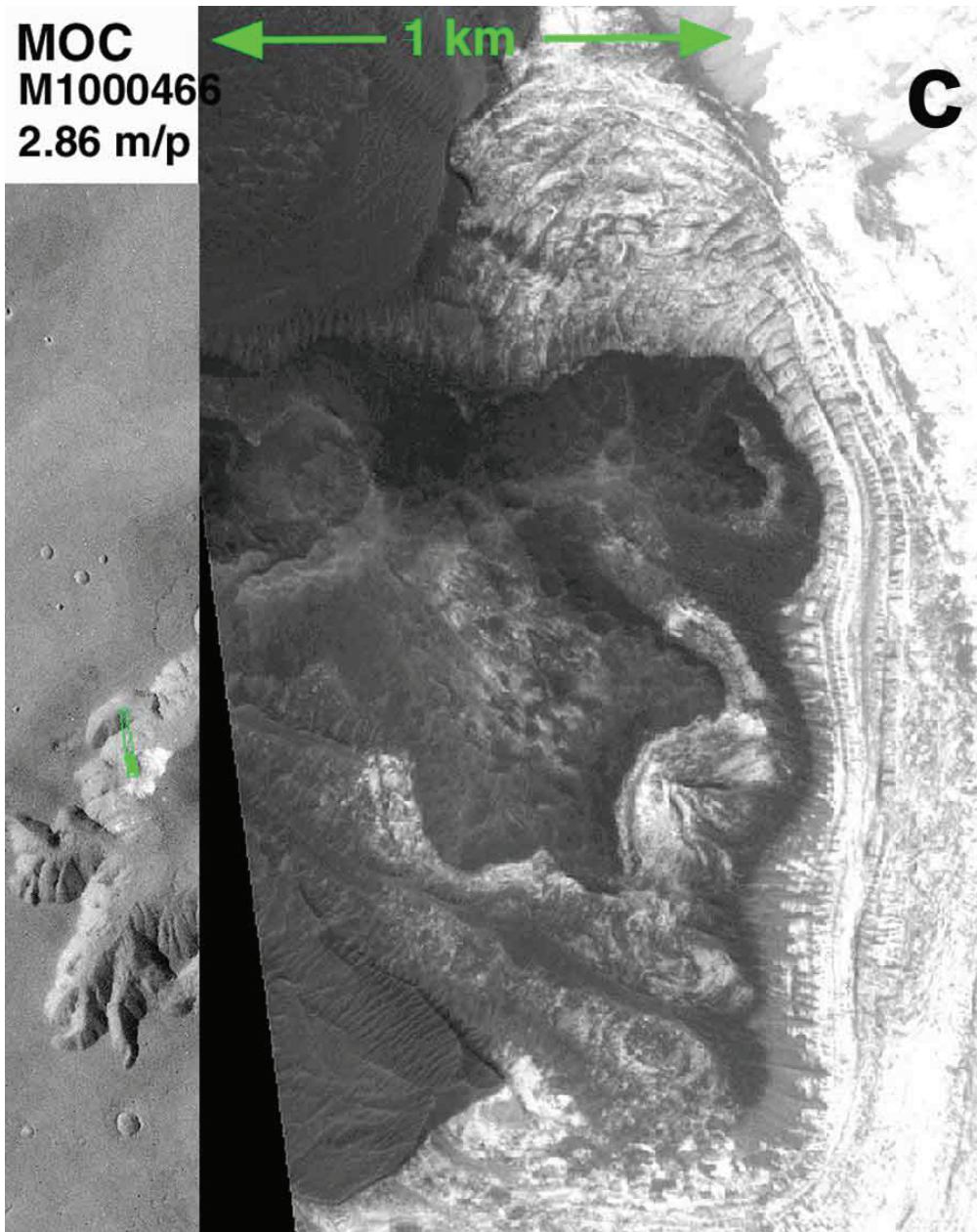


Figure 18c & 18d: (c) Dark material in MOC 100046 (courtesy Malin Space Science Systems) shows cone-like feature superposed on ILD in Juventae Chasma (Chapman and Smellie, 2001); (d) Dark material in MOC 806284 (courtesy Malin Space Science Systems) shows possible dike and maar-like cones superposed on ILD in west Candor Chasma (Chapman, 2002).

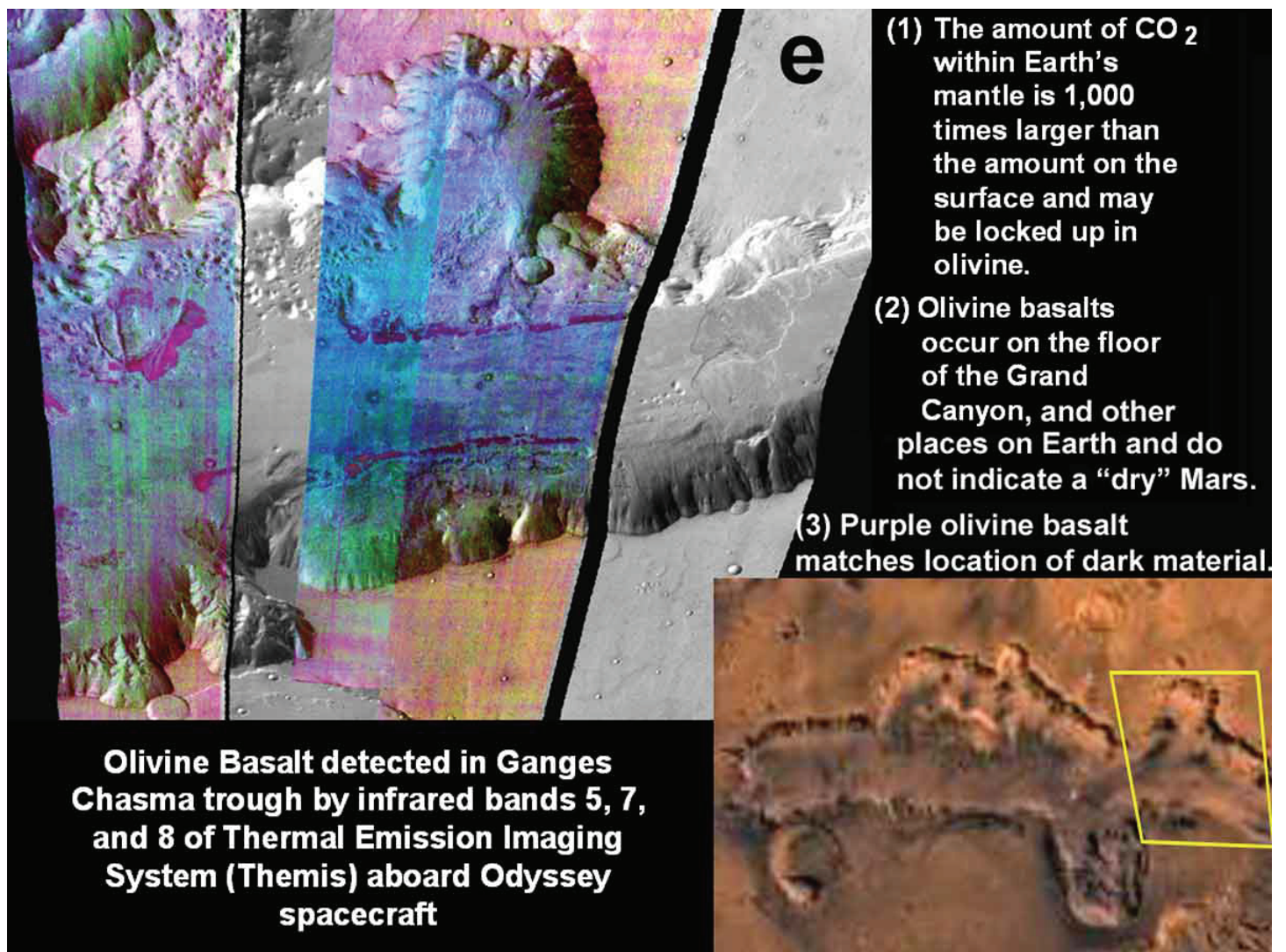


Figure 18e: Dark material may be olivine basalt (courtesy Themis Team).

Figure 19: Hypothetical scenario that may account for sub-ice volcanism in Valles Marineris, local features, and materials. (a) Proto-Valles Marineris extension due to rise of magma in the Late Noachian forms initial rifts and grabens (in red) that drain subsurface water downslope into Xanthe and Margaritifer Terra; (b) Fissure eruptions and caldera collapse (sub-circular to oval sections of Valles Marineris), in Late Noachian to Early Hesperian, generate widespread ignimbrites that bury ice rich materials downslope (possible buried fissures indicated by dotted lines); (c) Continued Hesperian rise of magma forces water into voids of Valles Marineris to freeze in depression ponds or in dammed areas upstream from ignimbrites, and lava erupted under ice forms sub-ice volcanoes (in green) or chaos (in orange), subsequent floods (shades of blue indicating varied ages), and covers ice with a blanket of protective ash; inset: Dec. 19, 1998 Grímsvötn subglacial eruption (Oddur Sigurdsson, photographer); (d) Late Hesperian to Early Amazonian eruptions east of Valles Marineris generate more chaos, ash, hydrothermal alteration, and continued flooding. Finally, Kasei Valles is covered by lava flows from Tharsis, the volcanic system shuts slowly down, glaciers eroded the ILDs, all ash-covered surface ice slowly sublimates, un-butressed water-inundated walls of Valles Marineris collapse to form locale landslides, small late-stage eruptions produce dark materials in Valles Marineris, gullies cut ILDs, and wind erosion/deposition alters surfaces (Chapman and Tanaka, 2002).

## References for Sub-ice Origin of ILDS

- Chapman, M.G., 2002, Layered, massive, and thin sediments on Mars: Possible Late Noachian to Late Amazonian tephra? in Smellie, J. L. & Chapman, M. G. (eds) Volcano--Ice Interactions on Earth and Mars. Geological Society, London, Special Publications, 202, 273-203.
- Chapman, M.G., 2003, Sub-ice volcanoes and ancient oceans/lakes: A Martian challenge, in Subglacial lakes' detection, outbursts mechanisms and consequences, Amir Moktari-Fard (Ed.), Special Paper on Subglacial Lake Detection, Global and Planetary Change 35, 185-198.
- Chapman, M. G. and J. L. Smellie, 2001. Putative large and small volcanic edifices in Valles Marineris, Mars and evidence of ground water/ice, (abs.) Eos Trans. AGU, Fall Meet. Suppl. P21C-11, F698.
- Chapman, M. G. and J. L. Smellie, in submission. Mars interior layered deposits and terrestrial sub-ice volcanoes compared: Observations and interpretations of similar geomorphic characteristics: in Chapman, M. G. & Skilling, I. P. (eds), The Geology of Mars: Evidence from Earth-Based Analogues, Cambridge University Press, Cambridge, U.K.
- Chapman, M. G. and K. L. Tanaka, 2001. The interior deposits on Mars: sub-ice volcanoes?. J. Geophys. Res. 106, 10,087-10,100.
- Chapman, M.G. and K.L. Tanaka, 2002, Related magma-ice interactions: Possible origin for chasmata, chaos, and surface materials in Xanthe, Margaritifer, and Meridiani Terra, Mars, Icarus v. 155, no. 2, 324-339. Chapman, M.G., M.T. Gudmundsson, A.J. Russell, T.M. Hare, 2003. Possible Juventae Chasma sub-ice volcanic eruptions and Maja Valles ice outburst floods, Mars: Implications of MGS crater densities, geomorphology, and topography. JGR-Planets 108, E10, 5113, 2(1)-2(20).
- Croft, S. K., 1990. Geologic map of the Hebes Chasma quadrangle, VM 500K 00077, (abs.) NASA TM 4210, 539-541.
- Komatsu, G., G. G. Ori, P. Ciarcelluti, and Y. D. Litasov, 2004. Interior layered deposits of Valles Marineris, Mars: Analogous subice volcanism related to Baikal Rifting, Southern Siberia, Planetary and Space Science 52, 167-187.
- Larsen, G. and S. Thorarinsson 1977: H-4 and other acid Hekla tephra layers. Jökull 27: 28-46. Lucchitta, B. K., Isbell, N. K. & Howington-Kraus, A. 1994. Topography of Valles Marineris: Implications for erosional and structural history. J. Geophys. Res. 99, 3783-3798. Sigvaldason, G. E. 1992. Recent hydrothermal explosion craters in an old hyaloclastite flow, central Iceland. J. Vol. & Geotherm. Res. 54, 53-63.
- Schopka, H.H., M.T. Gudmundsson and S.P. Jakobsson. 2003. Formation of Helgafell, SW-Iceland. Ice-volcano interaction during a fissure eruption under glacier and the effect of ice cap geometry on distribution of erupted products (In Icelandic). The Geoscience Society of Iceland Spring Meeting 2003, abstracts, 36-37.